university of groningen / faculty of science and engineering

Electrostatic complexation between oppositely charged block-type glycopolymers

Master Thesis Chemistry

March 2, 2021

Author:

Joël Benninga

Supervisors:

prof. dr. Katja Loos

dr. Théophile Pelras

Maryam Bozorg, MSc

Zernike Institute for Advanced Materials

Macromolecular Chemistry and New Polymeric Materials group

ABSTRACT

Glycopolymers (*i.e.* macromolecules bearing pendant saccharide units) have attracted considerable attention, particularly in the field of drug delivery, due to their biocompatibility and capability of molecular recognition with lectins. Furthermore, glycopolymers can be produced from naturally occurring sugars and in a controlled fashion with tailored molecular weight, structure, functionality, and even sequencing. Although glycopolymer self-assembly and even drug delivery have been reported before, only one article has been published on the self-assembly of oppositely charged glycopolymers. The electrostatic interactions of polyelectrolytes – macromolecules carrying multiple charges – often dictate their physical properties, including self-assembly. When two oppositely charged polyelectrolytes are mixed in solution, interpolyelectrolyte complexes are typically formed due to cooperative electrostatic interactions. Therefore, the goal of this master's thesis was to explore the formation of glycosylated nanoparticles through electrostatic interactions between block-type glycopolymers of opposite charges.

First, a glycomonomer was synthesised by selectively attaching an acrylate functionality onto a hydroxy group in glucose. This glycomonomer was subsequently used to produce a glycopolymer via reversible addition-fragmentation chain transfer (RAFT) polymerisation using a trithiocarbonate chain transfer agent. Then, the glycopolymer with the chain transfer agent still attached on was used for chain extension with two different monomers yielding block-type glycopolymers: protected poly(glucose acrylate)-*block*-poly(*tert*-butyl acrylate) and protected poly(glucose acrylate)-*block*-poly(dimethylaminopropyl acrylamide). Next, these block copolymers were modified with deprotection reactions, and a quaternisation, yielding negatively charged poly(glucose acrylate)-*block*-poly(acrylic acid) and positively charged poly(glucose acrylate)-*block*-poly(quaternised dimethylaminopropyl acrylamide). Finally, the modified block-type glycopolymers were dissolved in a phosphate buffer at pH 12 and mixed with one another to allow for electrostatic complexation. A significant increase in average particle size was observed with dynamic light scattering. In addition, atomic force microscopy revealed nanoparticles of similar dimensions. These findings were ascribed to the electrostatic self-assembly of the glycopolymers into spherical micelles, achieving the goal of this master's thesis.

This research can be expanded upon by, for example, investigating whether the self-assembled micelles are suitable for drug delivery. A start would be to determine the reversibility of the electrostatic complexation. Once reversible aggregation of the nanoparticles has been achieved the next step would be to confirm and measure the extent of drug loading. Finally, drug delivery into, for example, isolated cancer cells could be studied.

PREFACE

This master's thesis was carried out at the University of Groningen within the Macromolecular Chemistry and New Polymeric Materials group between August 2020 and March 2021. I wish to thank prof. dr. Katja Loos for her supervision and for giving me the opportunity to do the master research project in her group.

I cannot thank dr. Théophile Pelras enough for his guidance and patience as daily supervisor. He was always open for scientific and non-scientific discussion, ranging from complex macromolecular structures to the latest film or television series. He taught me a great deal about polymer synthesis and characterisation, for which I am very grateful.

I would also like to thank the VvP (the polymer chemists' association) for organising great activities that gave me the opportunity to mingle and meet its members outside of working hours.

Lastly, I want to thank all group members for the great and welcoming atmosphere.

Groningen, 24th of February, 2021

Joël Benninga

Contents

ABSTRACT ..... **I**
PREFACE ..... **II**
ABBREVIATIONS ..... **V**
1 INTRODUCTION **1**
1.1 RAFT polymerisation 1
1.2 Amphiphilic block copolymers 3
1.3 Self-assembly of block copolymers 4
1.4 Interpolyelectrolyte complexes 6
1.5 Glycopolymers 7
1.6 Self-assembly of glycopolymers 8
1.7 Goal 9
1.8 Approach 10
2 MATERIALS AND METHODS **13**
2.1 Materials 13
2.2 Characterisation techniques 14
2.3 Synthesis 15
2.3.1 Monomers 15
2.3.2 Homopolymers 16
2.3.3 Block copolymers 17
2.3.4 Polymer modifications 18
3 RESULTS AND DISCUSSION **20**
3.1 Synthesis of glycomonomers 20
3.2 Synthesis of block-type glycopolymers from dithiobenzoate RAFT agent 23
3.3 Synthesis of block-type glycopolymers from trithiocarbonate RAFT agent 26
3.4 Polymer self-assembly 31
4 CONCLUSIONS AND OUTLOOK **35**
5 REFERENCES **37**
6 SUPPORTING INFORMATION **41**
6.1 ^{13}C-NMR spectra of glycomonomer synthesis 41
6.2 HRMS spectra of glycomonomers 42
6.3 ^{1}H-NMR spectra of the deprotection of P*t*BA and Pr-PGA with TFA or HFIP 43

6.4 ζ-potential measurements 44
6.5 AFM data 46

ABBREVIATIONS

^{13}C-NMR	Carbon nuclear magnetic resonance spectroscopy
^{1}H-NMR	Proton nuclear magnetic resonance spectroscopy
AFM	Atomic force microscopy
AIBN	Azobisisobutyronitrile
ATRP	Atom transfer radical polymerisation
BA	*n*-Butyl acrylate
$CDCl_3$	Chloroform-*d*
CPBD	2-Cyano-2-propyl benzodithioate
CTA	Chain transfer agent
Đ	Dispersity
D_2O	Deuterium oxide
DCM	Dichloromethane
DDMAT	2-(Dodecylthiocarbonothioylthio)-2-methylpropionic acid
DI water	Deionised water
DLS	Dynamic light scattering
DMAEMA	Dimethylaminoethyl methacrylate
DMAPAA	Dimethylaminopropyl acrylamide
DMF	*N,N*-Dimethylformamide
DMSO-d_6	Dimethyl sulfoxide-d_6
DP	Degree of polymerisation
ESI	Electrospray ionisation
Et_2O	Diethyl ether
H_2SO_4	Sulphuric acid
HCl	Hydrochloric acid
HEA	2-Hydroxyethyl acrylate
HFIP	Hexafluoroisopropanol
HRMS	High-resolution mass spectrometry
IPEC	Interpolyelectrolyte complex

LAMs	Less activated monomers
MAMs	More activated monomers
MeI	Iodomethane
$MgSO_4$	Magnesium sulphate
M_n	Number average molecular weight
$Na_2HPO_4{\cdot}7H_2O$	Sodium phosphate dibasic heptahydrate
NABG	*N*-(4-aminobutyl)-D-gluconamide
NaCl	Sodium chloride
NaOH	Sodium hydroxide
PAA	Poly(acrylic acid)
PBA	Poly(butyl acrylate)
PDMAEMA	Poly(dimethylaminoethyl methacrylate)
PDMAPAA	Poly(dimethylaminopropyl acrylamide)
PDMAPAA-Q	Poly(quaternised dimethylaminopropyl acrylamide)
PGA	Poly(glucose acrylate)
PHEMAGI	Poly(2-{[D-glucosamin-2-*N*-yl)carbonyl]oxy}ethyl methacrylate)
Pr-G	Protected glucose
Pr-GA	Protected glucose acrylate
Pr-GMA	Protected glucose methacrylate
Pr-PGA	Protected poly(glucose acrylate)
Pr-PGMA	protected poly(glucose methacrylate)
P*t*BA	Poly(*tert*-butyl acrylate)
P*t*BMA	Poly(*tert*-butyl methacrylate)
RAFT	Reversible addition-fragmentation chain transfer
RDRP	Reversible deactivation radical polymerisation
SANS	Small-angle neutron scattering
SAXS	Small-angle X-ray scattering
SEC	Size-exclusion chromatography
SI	Supporting information

*t*BA	*tert*-Butyl acrylate
*t*BMA	*tert*-Butyl methacrylate
TEA	Triethylamine
TEM	Transmission electron microscopy
TFA	Trifluoroacetic acid
THF	Tetrahydrofuran
UV-Vis	Ultraviolet-visible spectroscopy

1 INTRODUCTION

Modern life cannot be imagined without polymers. While initially introduced for commodity applications as mediocre duplicates of natural materials such as ivory, polymers have recently found applications in a vast range of technologies, for example, biomedicine, microelectronics and nanotechnology.[1] Still, the range of possibilities is very limited when considering linear polymers of homogeneous composition (also referred to as homopolymers). This has encouraged the development of more complex structures, which can only be achieved through the precise assembly of building blocks.[2] While living anionic[3] and cationic[4] polymerisation techniques are well-established and permit the synthesis of macromolecules with remarkable precision, their high sensitivity towards solvent impurities and incompatibility with nucleophilic monomers have stimulated the development of more robust and versatile controlled polymerisation techniques. These techniques have enabled the formation of multiblock polymers that allow the precise build-up of structured soft matter.[2]

1.1 RAFT polymerisation

One of these controlled polymerisation techniques is the reversible addition-fragmentation chain transfer (RAFT) process: a very well-known technique that was first reported in 1998.[5] RAFT is part of the reversible deactivation radical polymerisation (RDRP) family, meaning it is a controlled radical polymerisation process that relies on the reversible capping of growing chains. This enables the synthesis of macromolecules with a predictable molecular weight (M_n), low dispersity (Đ), high end-group fidelity, and capacity for continued chain growth.[6]

Advantages of RAFT include its simplicity, low cost, and compatibility with a wide range of monomer types (*e.g.* (meth)acrylates and (meth)acrylamides) and functionalities, including unprotected nucleophiles (*e.g.* acids, primary and secondary amines, hydroxy groups and nitriles). Furthermore, RAFT allows the tuning of the polymerisation rate and number fraction of living chains. This is done by controlling the number of radicals initially introduced in the system, as this directly corresponds to the number of chains that may undergo bimolecular termination. RAFT can also offer some benefits with respect to conventional free radical polymerisation for the polymerisation of certain monomers (*e.g.* ethylene and dienes). A problem with the free radical polymerisation of ethylene is branching due to backbiting, which leads to high molecular weight materials with large Đ. The polymerisation of dienes (such as butadiene and isoprene) using a free radical technique usually leads to cross-linking early in the reaction. The use of RAFT with specific reaction conditions, however, results in a more favourable outcome. For polyethylene lower Đ is reached due to reduced branching reactions. Furthermore, chain extension is made possible. In the case of dienes much

higher conversions can be reached before cross-linking stops the reaction via gelation of the system.[6]

RAFT is based on an equilibrium between active and dormant chains, of which the mechanism is shown in Figure 1.[6] After initiation (step I) the radical reacts with a monomer to form a polymeric radical with n monomer units (step II). The polymeric radical adds to the chain transfer agent (CTA, also referred to as RAFT agent) establishing an equilibrium between active and dormant polymer species (steps III and V). In an ideal process this equilibrium ensures that all chains have a similar degree of polymerisation (DP), as the rate of formation of dormant species is higher than the rate of propagation.[6]

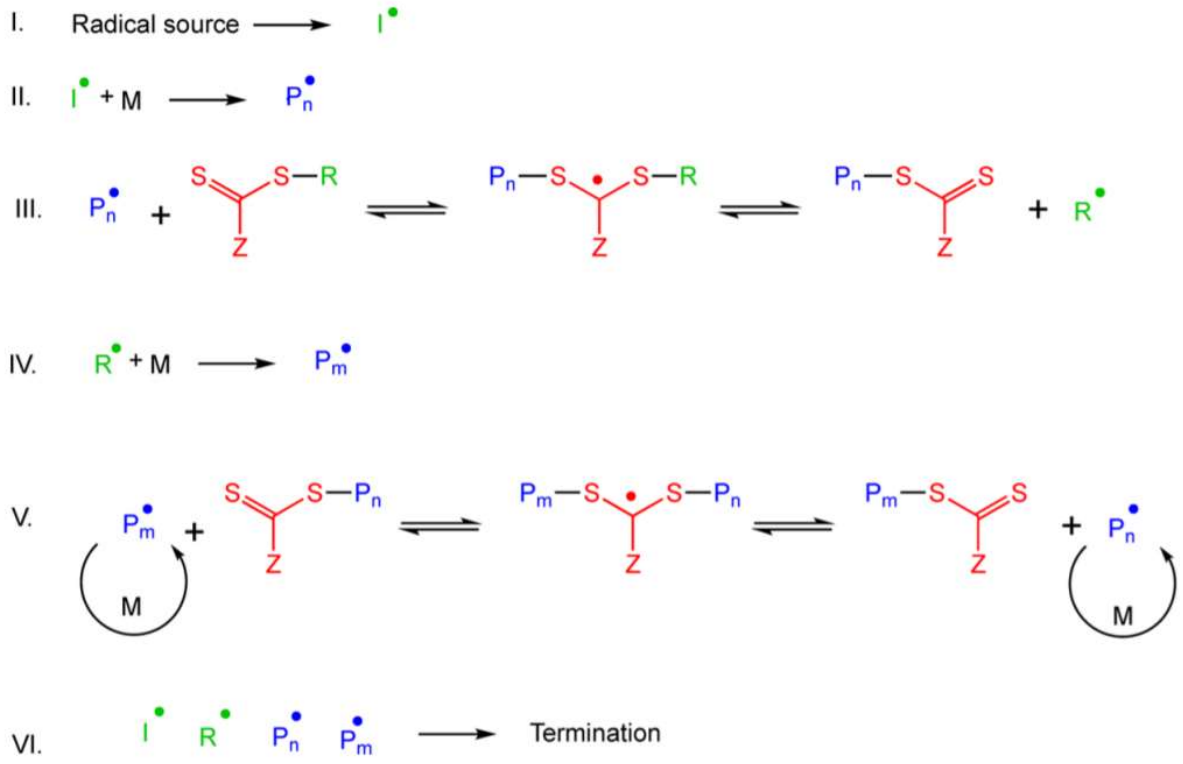

Figure 1: RAFT reaction mechanism, reproduced from reference 6.

A slight disadvantage lies in the selection of the RAFT agent. In addition to the type of monomer being polymerised, one has to account for the reaction conditions, and the monomers used for chain extension. For example, monomers containing nucleophilic substituents such as primary and secondary amines may interfere with polymerisation by undergoing side reactions with the thiocarbonylthio group of the RAFT agent.[7] This can be solved, however, by tuning the reaction conditions.[6] A few examples of RAFT agents are presented in Figure 2. RAFT agents such as dithioesters (**1**) or trithiocarbonates (**2**) are suitable for controlling the polymerisation of 'more

activated' monomers (MAMs) but inhibit the polymerisation of 'less activated' monomers (LAMs). MAMs include styrene, acrylamide, acrylonitrile and methyl (meth)acrylate, while LAMs are, for example, vinyl acetate, *N*-vinylcarbazole and *N*-vinylpyrrolidone. RAFT agents such as xanthates (**3**), on the other hand, are ineffective for controlling polymerisations of MAMs but can be suitable for LAMs.[8]

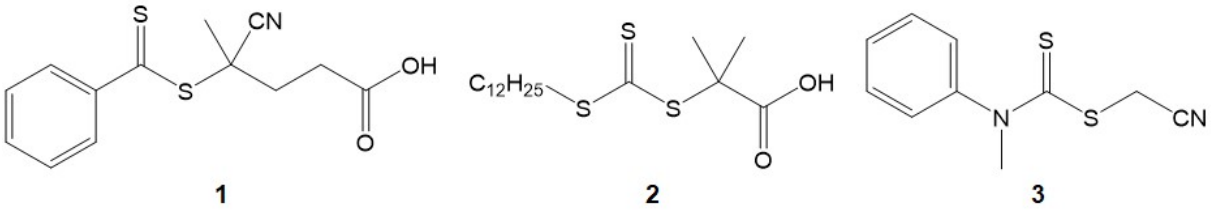

*Figure 2: Chemical structures of RAFT agents, **1**: 4-cyano-4-(phenylcarbonothioylthio)pentanoic acid, **2**: 2-(dodecylthiocarbonothioylthio)-2-methylpropionic acid, **3**: cyanomethyl methyl(phenyl)carbamodithioate.*

1.2 Amphiphilic block copolymers

RAFT and other controlled polymerisation techniques have enabled the formation of polymers that allow the precise build-up of structured soft matter. However, the self-assembly of linear homopolymers (*i.e.* polymers that comprise of a single monomer type throughout their chain) remains largely limited in spite of tailored chemical composition, molecular weight and chain-ends permitted by these techniques. The introduction of a second block of a different nature, though, opens doors for the directed formation of nanostructures. Macromolecules that consist of two or more covalently linked blocks of different polymerised monomers are called block copolymers. When these copolymers consist of a hydrophilic block linked to a hydrophobic block they are called amphiphilic block copolymers (Figure 3). Amphiphilic block copolymers are of great interest owing to their capability to self-assemble into several architectures due to their unique chemical structure. Applications include in fields such as materials science and biomedicine, but also consumer products (*e.g.* paints, textile and cosmetics).[9]

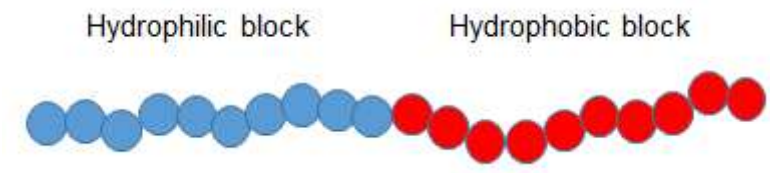

Figure 3: Schematic of an amphiphilic block copolymer.

1.3 Self-assembly of block copolymers

The self-assembly of amphiphiles is ubiquitous in nature and even in daily life: phospholipids self-assemble to form membranes of living cells, while the self-assembly of small-molecule surfactants gives rise to soap bubbles.[10-11] Diverse morphologies have been obtained by the self-assembly of amphiphilic block copolymers in solution. For certain diblock copolymers with chemically incompatible blocks the volume fraction of each block can be tuned to yield spheres, cylinders, or lamellae (Figure 4).[12]

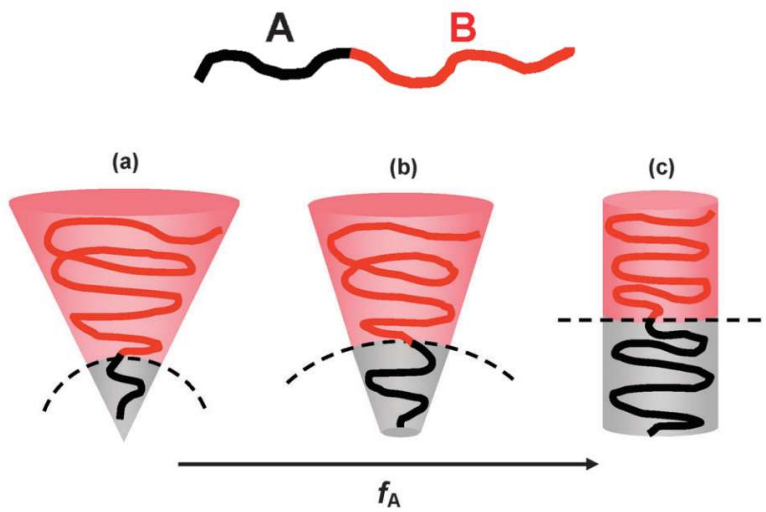

Figure 4: Schematic illustration of the different morphologies of AB diblock copolymers in solution changing from sphere (a) to cylinder (b) and to lamella (c) with increasing volume fraction (f_A) of the A block. Adapted from reference 12.

Similarly, in bulk, diblock copolymers with immiscible blocks can yield ordered structures in a wide range of morphologies, including spheres (S), cylinders (C), gyroids (G), and lamellae (L), as seen in Figure 5a. The process is driven by an unfavourable mixing enthalpy coupled with a small mixing entropy, while macroscopic phase separation is prevented by the covalent bond connecting the blocks. The microphase separation of diblock copolymers, *i.e.* the segregation of the two blocks within a polymer chain, depends on the total degree of polymerisation N, the volume fraction f of each block, and the Flory-Huggins parameter χ (*i.e.* the degree of incompatibility between the blocks). The segregation product, χN, determines the degree of microphase separation of diblocks, where $\chi N < 10$ is known as the weak segregation limit, and $\chi N >> 10$ is known as the strong segregation limit.[12]

Theories have been developed to describe the phase behaviour of diblock copolymers in bulk. One of them is the self-consistent mean-field theory, with which a phase diagram of diblock copolymers

has been predicted (Figure 5b).[12] Within the weak segregation limit the system is in a disordered (*i.e.* homogeneous) state. In the strong segregation limit with increasing f_A the copolymers undergo various order-to-order transitions starting from disorder passing through (closely packed) spheres, cylinders, gyroids, to lamellae depending on the segregation product (~ 10.5 < χN < ~ 60). As f_A increases from 0.5 to 1, the transitions are inverted with block B morphing into the aforementioned structures.[12]

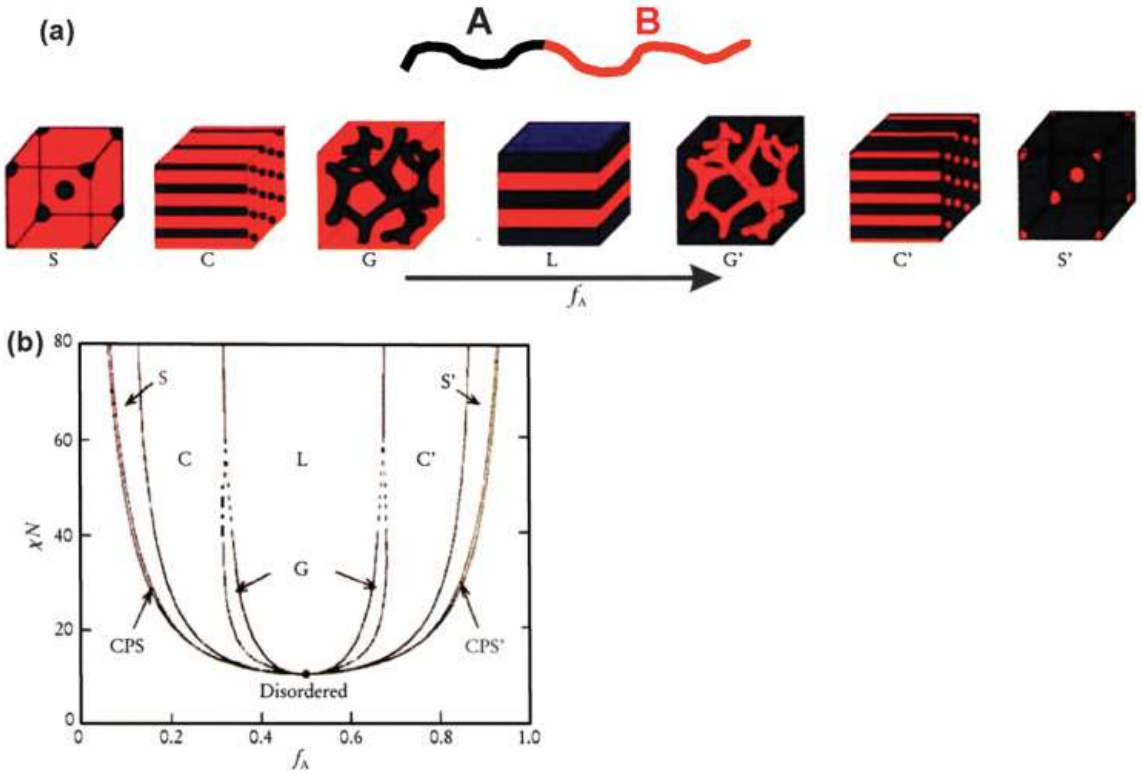

Figure 5: (a) Equilibrium morphologies of diblock copolymers in bulk: S and S' = spheres, C and C' = cylinders, G and G' = gyroids, L = lamellae. (b) Theoretical phase diagram of diblock copolymers in bulk predicted by the self-consistent mean-field theory, depending on volume fraction (f) of the blocks and the segregation parameter (χN), where χ is the Flory-Huggins parameter and N is the total degree of polymerisation; CPS and CPS' = closely packed spheres, reproduced from reference 12.

To give an idea of the complexity of block copolymer self-assembly in solution: the self-assembly of polystyrene-*block*-poly(acrylic acid) (PS-*b*-PAA) in solvent-nonsolvent mixtures involves six χ-parameters. In addition to the χ-parameter describing the incompatibility between blocks, now χ-parameters are needed to describe the compatibility between solvent and nonsolvent (*i.e.* selective solvent for one of the blocks), and their individual compatibility with each block. When a nonsolvent, such as water, is added to a solution containing amphiphilic diblocks, usually the first aggregates to form are spherical micelles. The hydrophilic coronas allow the micelles to dissolve in water, while

the hydrophobic cores provide an ideal location for encapsulation of, for example fluorescence probes, genes, proteins, or hydrophobic drugs.[12]

1.4 Interpolyelectrolyte complexes

While the solution and bulk self-assembly of amphiphilic block copolymers are useful and versatile ways to produce nanoparticles and nanostructures, another approach exists for the production of soft matter, namely interpolyelectrolyte complexation. The electrostatic interactions of polyelectrolytes – macromolecules carrying multiple charges – often dictate their physical properties, including self-assembly.[13] When two oppositely charged polyelectrolytes are mixed in solution, interpolyelectrolyte complexes (IPECs) are typically formed (Figure 6) due to cooperative electrostatic interactions. These complexes were proposed to consist of ordered ("ladder-like") domains and disordered ("scrambled egg") domains. Although hydrogen bonding and hydrophobic interactions may play a role in complexation, the main driving force in aqueous media is the entropy gain for the system due to the release of counterions associated with the charged groups on the polyelectrolytes.[13]

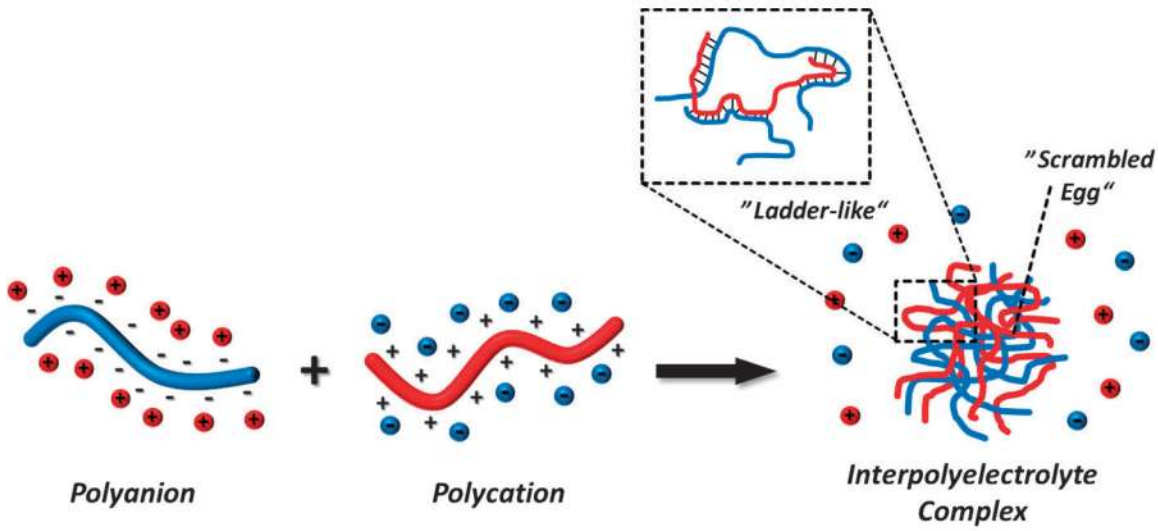

Figure 6: Schematic illustration of interpolyelectrolyte complex (IPEC) formation from polyanions and polycations, reproduced from reference 13.

Polyelectrolytes were traditionally used in the field of drug delivery, for example as carrier for anticancer drugs[14], or for complexation with charged genetic material like small interfering RNA[15] or plasmid DNA[16], but their use has now moved towards nanomaterials and engineering with the precise formation of nanostructures and multi-layered particles.[17-18] A great benefit of IPECs is their dynamic nature. Increasing the ionic strength of a solution containing IPECs leads to their complete

breakup, while subsequent reduction of ionic strength can restore the IPEC morphology.[17] In the case of weak polyelectrolytes (*i.e.* polyelectrolytes that are only charged within a certain pH range), the solution pH strongly influences the extent of interpolyelectrolyte complexation.[19] Additionally, structural changes of IPECs due to temperature have also been reported.[20-21] Moreover, different IPEC morphologies at the same final conditions have even been observed through pathway-dependent micelle preparation.[22]

Interpolyelectrolyte complexes have shown great potential in biomedical applications such as synthetic cartilage and as carriers of therapeutics (*e.g.* drugs, proteins, or nucleic acids).[23]

1.5 Glycopolymers

While polyelectrolytes and amphiphilic block copolymers are interesting candidates for drug delivery applications, one challenge is to selectively target the carrier to the site of interest *in vivo*. A way to tackle this problem might be by incorporating carbohydrate moieties in the hydrophilic corona of micelles formed from self-assembled block copolymers. It has been demonstrated that specific carbohydrates, such as glucose, enhance the delivery into bacteria or macrophages, due to their involvement in many molecular recognition events, and presence on nearly every cell surface. These recognition processes are based on specific and noncovalent interactions between carbohydrates and proteins. While this interaction is typically weak, simultaneous multivalent interactions originating from the high number of glycosyl groups along a polysaccharide, add up and result in a strong attraction between carbohydrates and proteins. This phenomenon is often referred to as the "cluster glycoside effect".[24]

Whilst naturally occurring polysaccharides* are highly abundant, they cannot be polymerised in a controlled fashion, and their processing is often hampered by their limited solubility and an inherent fragility. Glycopolymers (*i.e.* macromolecules bearing pendant saccharide units) have therefore been developed as an alternative. Furthermore, glycopolymers can be produced from naturally occurring sugars, and in a controlled fashion with tailored molecular weight, structure, functionality, and even sequencing.[26] A few examples of glycopolymers (**1**-**3**) and a polysaccharide (**4**) are shown in Figure 7.[27-28] Note that there is a difference between polysaccharides and glycopolymers: for polysaccharides, carbohydrates are part of the polymer backbone, whereas for glycopolymers, carbohydrates are moieties attached to the polymer backbone.

* For a detailed account of polysaccharide-containing block copolymers the reader is referred to a recent review on their synthesis and applications.[25]

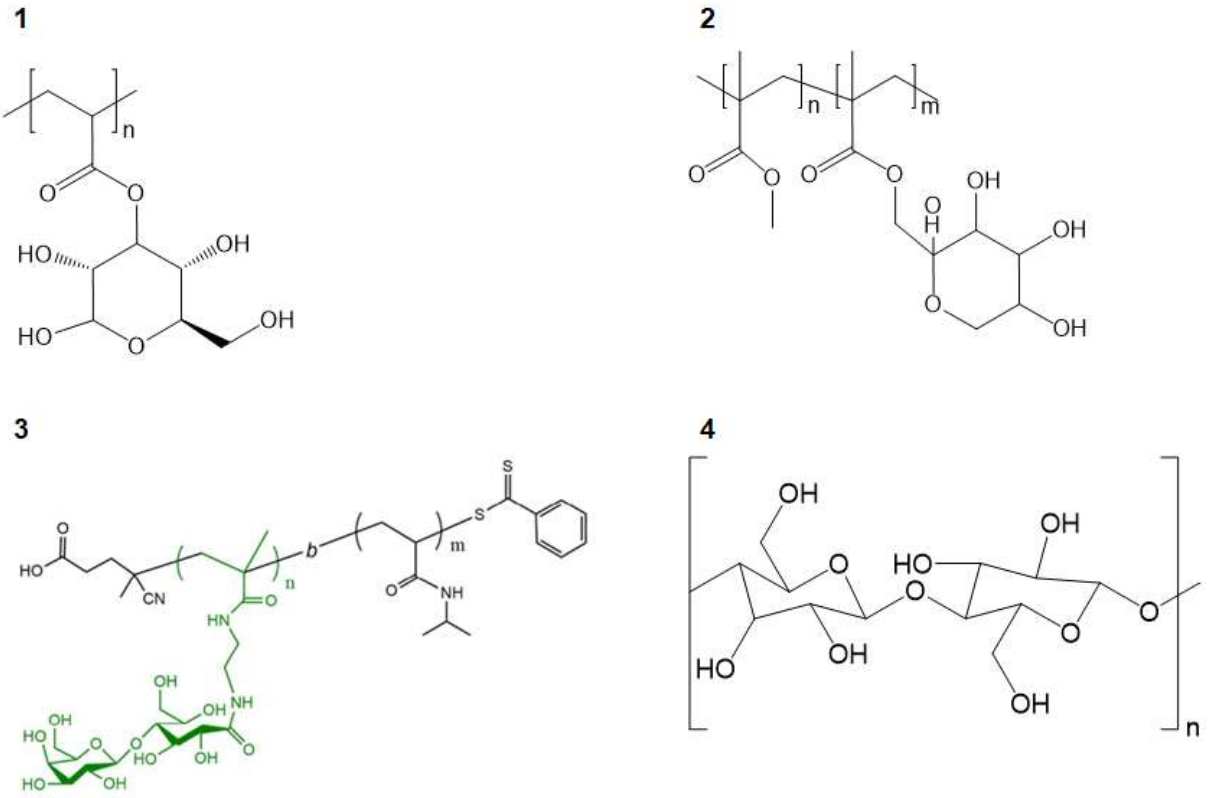

*Figure 7: Chemical structures of (glyco)polymers, **1**: poly(glucose acrylate), **2**: poly(methyl methacrylate)-block-poly(fructose methacrylate)[27], **3**: poly(2-lactobionamidoethyl methacrylamide)-block-poly(N-isopropylacrylamide)[28], **4**: cellulose.*

1.6 Self-assembly of glycopolymers

In literature there have been some reports on glycopolymer self-assembly. Fernández-García *et al.* studied the self-assembly of two well-defined diblock and triblock glycopolymers by dynamic light scattering and transmission electron microscopy (TEM). The glycopolymers in question were poly(butyl acrylate)-*block*-poly(2-{[D-glucosamin-2-*N*-yl)carbonyl]oxy}ethyl methacrylate) (PBA-*b*-PHEMAGI) and PHEMAGI-*b*-PBA-*b*-PHEMAGI, and were synthesised using atom transfer radical polymerisation (ATRP). The glycopolymers formed coexisting spherical micelles and polymeric vesicles in aqueous solution. Additionally, they investigated the biomolecular recognition capacity of these micelles and vesicles, using a lectin which specifically interacts with glucose groups: Concanavalin A, *Canavalia Ensiformis*. They showed that the binding capacity increases with the length of the HEMAGI glycopolymer segment in the block copolymer, while the architecture of the polymers did not seem to affect the lectin recognition process.[24]

In a more recent study, the same authors prepared amphiphilic glycopolymers by chemical modification of block copolymers based on 2-hydroxyethyl acrylate (HEA) and *n*-butyl acrylate (BA). They synthesised PBA-*b*-PHEA and PHEA-*b*-PBA-*b*-PHEA using ATRP, prior to incorporation of D-(+)-glucosamine or *N*-(4-aminobutyl)-D-gluconamide (NABG) by chemical modification of the HEA units. The glycopolymers microphase separated, leading to different morphologies as a function of block copolymer composition according to small-angle X-ray scattering (SAXS) experiments. Furthermore, it was shown that the water-soluble glycopolymers bearing D-(+)-glucosamine units aggregate due to selective interactions with the Concanavalin A lectin.[29]

Stenzel *et al.* loaded nanoparticles self-assembled from a block-type glycopolymer with the drug curcumin. They showed that curcumin was unexpectedly located in the shell of the micelle and that it lead to changes in morphology during self-assembly. These results were surprising since it is often assumed that a drug has no effect on the properties of a carrier, and that a hydrophobic drug will be entrapped in the hydrophobic core of a micelle. They added different amounts of curcumin to poly(1-O-methacryloyl -β-D-fructopyranose)-*block*-poly(methyl methacrylate), Poly(1-O-MAFru)$_{36}$-*b*-PMMA$_{192}$ and analysed the resulting self-assembled nanoparticles with TEM, SAXS, and small-angle neutron scattering (SANS). It was observed that the morphology of the nanoparticles changed from cylindrical micelles to polymersomes upon addition of curcumin, due to interactions with the glycopolymer block. The level of hydration of the shell was affected as well: increasing the amount of drug dehydrated the nanoparticle shell, coinciding with a lower nanoparticle uptake by breast cancer cells.[27]

Though glycopolymer self-assembly – and even drug delivery – has been reported before, this has been done using non-charged glycopolymers. There is one paper, however, that described the self-assembly of glycopolymers with zinc complexes to form positively charged nanoparticles, and successive electrostatic complexation of glycopolymers with these nanoparticles.[30] To the best of our knowledge, there is no other published work on the self-assembly of oppositely charged glycopolymers.

1.7 Goal

Therefore, the main goal of this master's thesis was to explore the formation of glycosylated nanoparticles through electrostatic interactions between block-type glycopolymers of opposite charges. The milestones of this thesis are outlined in Figure 8: glycomonomer synthesis starting from D-(+)-glucose, synthesis of oppositely charged block-type glycopolymers via RAFT polymerisation, and observation of their subsequent electrostatic self-assembly. Although non-

charged, it was not certain whether the glycopolymer segments would avoid parasitic interactions and permit controlled self-assembly.

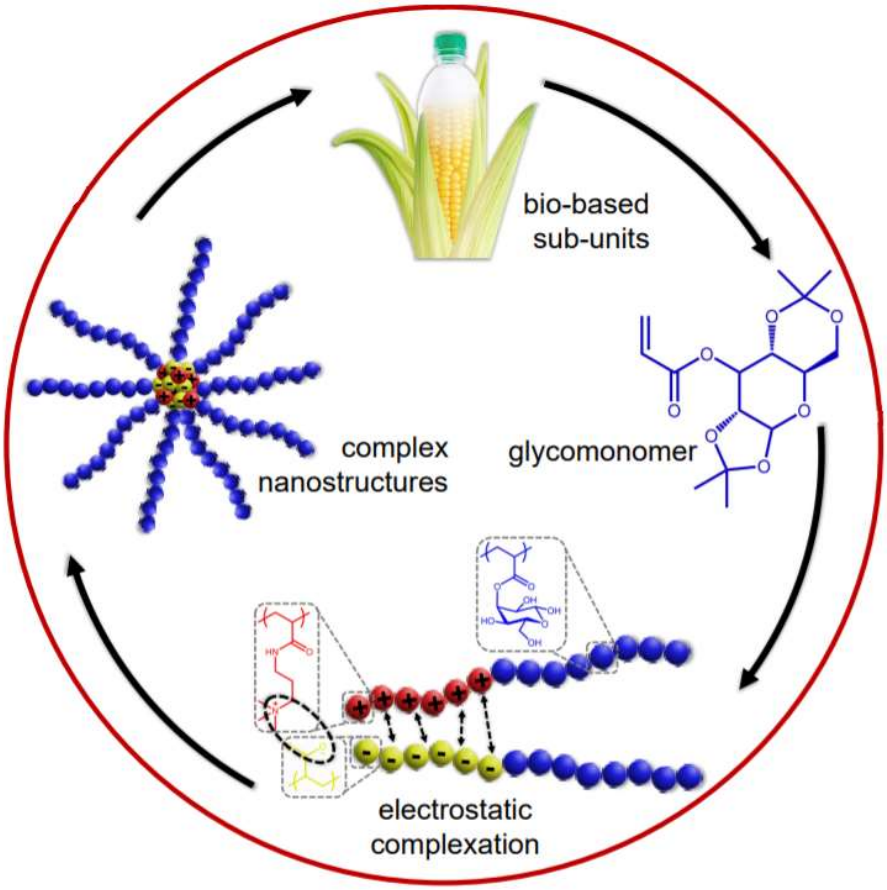

Figure 8: Steps towards the formation of glycosylated nanostructures, reproduced from reference 31.

1.8 Approach

The steps towards creating complex nanostructures from D-(+)-glucose are detailed below and shown schematically in Figure 9. Steps 'a' to 'd' relate to Figure 9a to 9d, respectively.

a. Synthesis of protected glucose acrylate glycomonomer (Pr-GA) and structure confirmation with proton and carbon nuclear magnetic resonance (^{1}H-NMR and ^{13}C-NMR) spectroscopy and high-resolution mass spectrometry (HRMS)
b. RAFT polymerisation of glycomonomer to form protected poly(glucose acrylate) homopolymer (Pr-PGA) and characterisation with ^{1}H-NMR and size-exclusion chromatography (SEC)
c. Chain extension of Pr-PGA with *tert*-butyl acrylate (*t*BA) to form protected poly(glucose acrylate)-*block*-poly(*tert*-butyl acrylate) (Pr-PGA-*b*-P*t*BA) and characterisation with ^{1}H-NMR and SEC.

Secondly, the removal of *tert*-butyl and acetonide protective groups to form PGA-*b*-PAA (PAA stands for poly(acrylic acid)) and characterisation with ^{1}H-NMR

d. Chain extension of Pr-PGA with dimethylaminopropyl acrylamide (DMAPAA) to form protected poly(glucose acrylate)-*block*-poly(dimethylaminopropyl acrylamide) (Pr-PGA-*b*-PDMAPAA) and characterisation with ^{1}H-NMR and SEC. Secondly, the removal of acetonide protective groups and then quaternisation of the amino group in the PDMAPAA block with iodomethane to form PGA-*b*-PDMAPAA-Q (Q stands for quaternised) and characterisation with ^{1}H-NMR
e. Charge-stoichiometric mixing of the polyelectrolytes and characterisation of the nanostructures with atomic force microscopy (AFM) and dynamic light scattering (DLS)

The deprotection reactions to form PGA-*b*-PAA are carried out to ensure that the polymer is charged and water-soluble at a high pH. The carboxylic acid moieties of the PAA block will then be deprotonated, and thus, negatively charged. Since PGA-*b*-PDMAPAA is not charged or water-soluble at this pH, a quaternisation is required on top of the deprotection reaction to yield PGA-*b*-PDMAPAA-Q, which is water-soluble and positively charged at any pH. The mixing of these charged and water-soluble block copolymers should induce the formation of IPECs. Although IPEC formation at an intermediate pH range is possible, it is very challenging and may result in only partially charged species.[32]

In the next chapter the experimental methods are described. In Chapter 3 the results and discussion can be found followed by the conclusions and outlook in Chapter 4. The references are listed in Chapter 5 and the thesis ends with the supporting information, which can be found in Chapter 6.

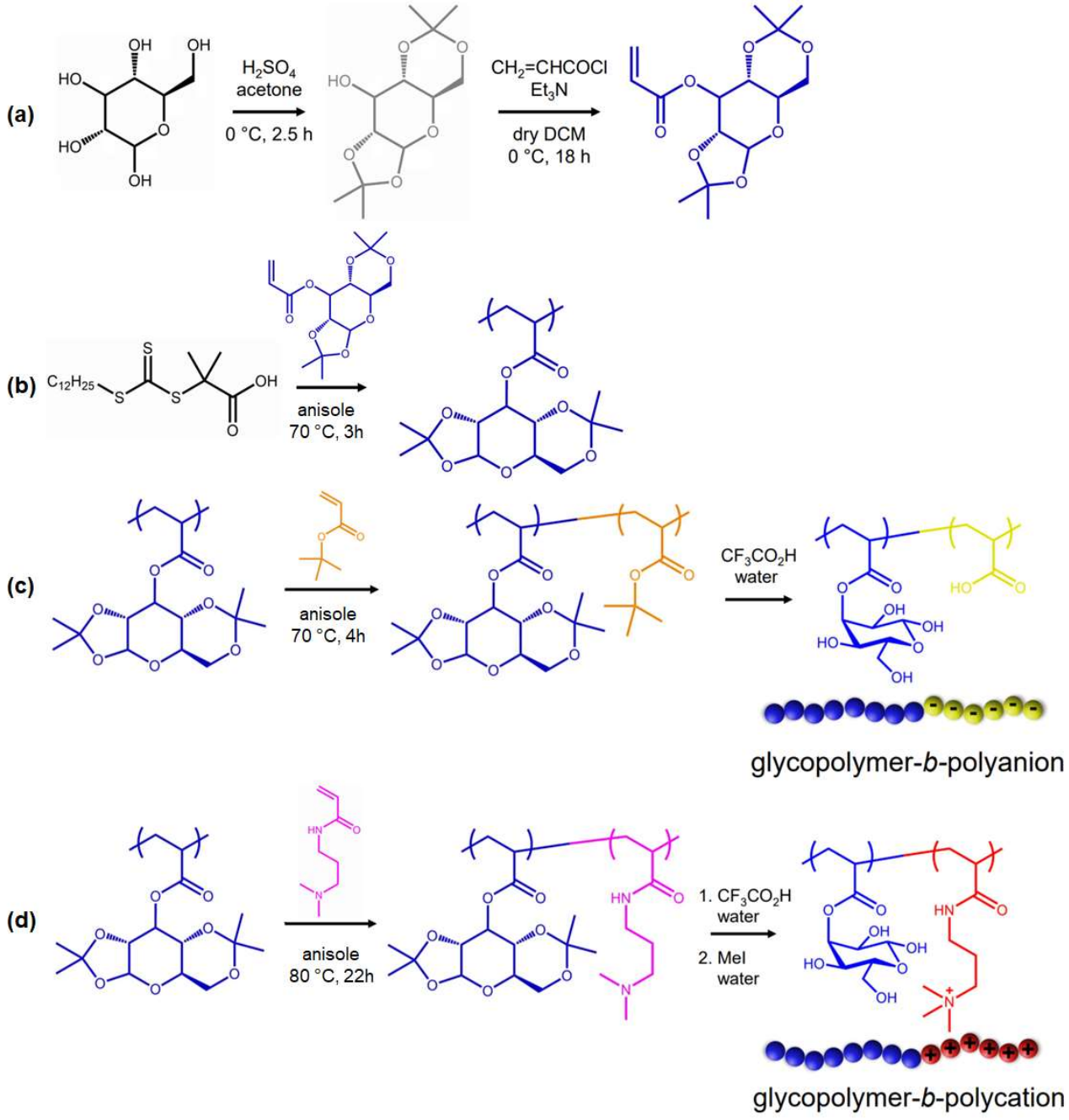

*Figure 9: (a) Synthesis of protected glucose acrylate glycomonomer (Pr-GA). (b) Synthesis of protected poly(glucose acrylate) (Pr-PGA) via RAFT polymerisation. (c) Synthesis of Pr-PGA-b-Pt*BA and subsequent deprotection to form PGA-*b*-PAA. (d) Synthesis of Pr-PGA-*b*-PDMAPAA and subsequent deprotection and quaternisation to form PGA-*b*-PDMAPAA-Q, reproduced from reference 31.

2 MATERIALS AND METHODS

2.1 Materials

The materials used for this thesis are listed below. AIBN was recrystallised from methanol, and monomers were passed through a short alumina column to remove inhibitors before polymerisation. All other materials were used as received.

- 1,4-Dioxane (Sigma-Aldrich, ≥ 99%)
- 2-(Dimethylamino)ethyl methacrylate, DMAEMA (Sigma-Aldrich, 98%)
- 2-(Dodecylthiocarbonothioylthio)-2-methylpropionic acid, DDMAT (Sigma-Aldrich, 98%)
- 2,2′-Azobis(2-methylpropionitrile), AIBN (Sigma-Aldrich, 98%)
- 2-Cyano-2-propyl benzodithioate, CPBD (Sigma-Aldrich > 97%)
- 4-Cyano-4-(phenylcarbonothioylthio)pentanoic acid, CTBPA (Sigma-Aldrich)
- Acetone (BOOM, HPLC grade)
- Acetonitrile (BOOM, HPLC grade)
- Acryloyl chloride (Sigma-Aldrich, ≥ 97%)
- Alumina (Sigma-Aldrich, activated basic, ≥ 98%)
- Anisole (Merck, for synthesis)
- Chloroform-*d*, $CDCl_3$ (Sigma-Aldrich, 99.8 atom % D)
- D-(+)-glucose (Sigma-Aldrich, ≥ 99.5%)
- Deionised water, DI water
- Deuterium oxide, D_2O (Sigma-Aldrich, 99.9 atom % D)
- Dichloromethane, DCM (Macron)
- Diethyl ether, Et_2O (Macron)
- Dimethyl sulfoxide-d_6, DMSO-d_6 (Sigma-Aldrich, ≥ 99.5 atom % D)
- Ethyl acetate (Macron)
- Hexafluoroisopropanol, HFIP (Sigma-Aldrich, ≥ 99%)
- Hexane (Macron, 99%)
- Hydrochloric acid, HCl (BOOM, 37-38%)
- Iodomethane, MeI (Sigma-Aldrich, 99%)
- Magnesium sulphate, $MgSO_4$ (BOOM, dried, extra pure)
- Methacryloyl chloride (Sigma-Aldrich, 97%)
- Milli-Q water, was obtained through a Labconco filtration system
- *N*-(3-Dimethylaminopropyl)acrylamide, DMAPAA (abcr, 98%)

- *N*,*N*-Dimethylformamide, DMF (Sigma-Aldrich, 99.8%)
- Sodium chloride, NaCl (Merck, for analysis)
- Sodium hydroxide, NaOH (ACROS Organics, extra pure pellets)
- Sodium phosphate dibasic heptahydrate, $Na_2HPO_4 \cdot 7H_2O$ (Sigma-Aldrich, ≥ 99.0%)
- Sulphuric acid, H_2SO_4 (BOOM, 95-97%)
- *tert*-Butyl acrylate, *t*BA (Sigma-Aldrich, ≥ 98.0%)
- *tert*-Butyl methacrylate, *t*BMA (Sigma-Aldrich, 98%)
- Tetrahydrofuran, THF (BOOM)
- Triethylamine, TEA (Sigma-Aldrich, ≥ 99.5%)
- Trifluoroacetic acid, TFA (Sigma-Aldrich, 99%)

2.2 Characterisation techniques

Proton nuclear magnetic resonance (^{1}H-NMR) spectra were recorded on an Agilent 400-MR 400 MHz spectrometer at 298 K. Chloroform-*d*, deuterium oxide or DMSO-d_6 were used as solvents to prepare samples (≈ 5 g L^{-1}). Regarding the measurement parameters, a pulse width of 45 µs, spectral width of 12/-2 ppm, recycle delay of 1 s and 16/32 scans were used. For glycopolymer samples, a pulse width of 90 µs, spectral width of 12/-2 ppm, recycle delay of 10 s and 64 scans were used. MestReNova software was used to analyse the spectra.

Size-exclusion chromatography (SEC) was performed on a Viscotek GPCMax system equipped with 302 TDA detectors array and two columns in series (Agilent Technologies PolarGel L and M, both 8 µm 30 cm). The columns and detectors were maintained at a temperature of 50 °C. DMF (Sigma-Aldrich, ≥ 99.9 %) containing 0.01 M lithium bromide was used as eluent at a flow rate of 1 mL min^{-1}. Near monodisperse PMMA standards from Polymer Standard Services were used for the construction of a calibration curve. Samples were dissolved in the eluent at a concentration of ≈ 3 g L^{-1} and passed through a 0.45 µm nylon filter prior to injection. Data acquisition and calculations were performed using Viscotek Omnisec software version 5.0.

High-resolution mass spectrometry (HRMS) was performed on an LTQ Orbitrap XL spectrometer (Thermo Fisher Scientific) with an ESI (electrospray ionisation) source. Samples were dissolved in DCM at a concentration of ≈ 1 g L^{-1} and passed through a 0.45 µm nylon filter prior to analysis.

Dynamic light scattering (DLS) experiments were performed using a Zetasizer Ultra (Malvern

Panalytical) equipped with a helium-neon laser operating at a wavelength of 633 nm. Samples were measured using a measurement angle of 90° and at a temperature of 298 K, and analysed with the ZS Xplorer software that uses an algorithm called Adaptive Correlation.

Tapping-mode atomic force microscopy (AFM) was performed on a Dimension 3100 system (Bruker) using NanoScope software. Samples were prepared by spin coating (4000 rpm, 60 s) a drop of charge-stoichiometric mixture of PGA_{98}-*b*-PAA_{37} and PGA_{98}-*b*-PDMAPAA-Q_{44} onto a freshly cleaned silicon wafer.

2.3 Synthesis

2.3.1 Monomers

Synthesis of Pr-G (glycomonomer precursor). D-(+)-glucose (10 g) was added to a round-bottom flask under 0 °C containing acetone (200 mL) and H_2SO_4 (10 mL). The mixture was stirred for 2 hours at room temperature. NaOH (30 g) in DI water (120 mL) was added to the mixture under 0 °C. Acetone was removed through evaporation. The mixture was extracted with DCM (3x 150 mL) and subsequently washed with DI water (3x 150 mL). $MgSO_4$ was added as drying agent, and then removed through Büchner filtration. The product was recrystallized in diethyl ether and hexane to yield a white crystalline solid.

Synthesis of Pr-GA (protected glucose acrylate). Pr-G (3 g, 11.5 mmol), triethylamine (2.4 ml, 17.3 mmol) and DCM (90 mL) were put in a round-bottom flask. Acryloyl chloride (1.4 ml, 17.3 mmol) was added dropwise at 0 °C under nitrogen flow. The mixture was left overnight at room temperature. DI water (~2 mL) was added to quench the reaction. DCM (60 mL) was added, and the mixture was washed with DI water (150 mL). DCM was removed through evaporation. Diethyl ether (150 mL) was added before washing with 0.1 M HCl (300 mL). The mixture was then washed with 0.1 M NaOH (300 mL) before washing with DI water (150 mL). $MgSO_4$ was added as drying agent, and then removed through Büchner filtration. Diethyl ether was removed through evaporation. A silica column was used to purify the product using an eluent ratio of 4:1 hexane : ethyl acetate to yield a transparent viscous oil that solidifies upon cooling.

Synthesis of Pr-GMA (protected glucose methacrylate). Pr-G (3 g, 11.5 mmol), triethylamine (2.4 ml, 17.3 mmol) and DCM (90 mL) were put in a round-bottom flask. Methacryloyl chloride (1.7 ml, 17.3 mmol) was added dropwise at 0 °C under nitrogen flow. The mixture was left overnight at room

temperature. DI water (~2 mL) was added to quench the reaction. DCM (60 mL) was added, and the mixture was washed with DI water (150 mL). DCM was removed through evaporation. Diethyl ether (150 mL) was added before washing with 0.1 M HCl (300 mL). The mixture was then washed with 0.1 M NaOH (300 mL) before washing with DI water (150 mL). $MgSO_4$ was added as drying agent, and then removed through Büchner filtration. Diethyl ether was removed through evaporation. A silica column was used to purify the product using an eluent ratio of 4:1 hexane : ethyl acetate to yield a transparent viscous oil that solidifies upon cooling.

2.3.2 Homopolymers

Synthesis of Pr-PGMA$_{89}$ (protected poly(glucose methacrylate)). CTBPA (10 mg, 36 µmol), Pr-GMA (1.18 g, 3.6 mmol), AIBN (0.59 mg, 3.6 µmol) and anisole (1.5 mL) were put in a Schlenk flask and bubbled with nitrogen gas for 15 min before the vessel was placed in an oil bath at 80 °C. After 3 hours the reaction mixture was cooled to room temperature and exposed to air. The mixture was precipitated in hexane before freeze-drying from acetonitrile. ^{1}H-NMR: conversion = 85 %, $M_{n,NMR}$ = 29 600 g·mol^{-1}, $M_{n,SEC}$ = 16 900 g·mol^{-1}, Đ = 1.24

Synthesis of PDMAEMA. CTBPA (20 mg, 72 µmol), DMAEMA (1.13 g, 7.2 mmol), AIBN (1.18 mg, 7.2 µmol) and anisole (3 mL) were put in a Schlenk flask and bubbled with nitrogen gas for 15 min before the vessel was placed in an oil bath at 70 °C. After 5 hours the reaction mixture was cooled to room temperature and exposed to air. No conversion was observed with ^{1}H-NMR. The mixture colour changed from pink to bright orange.

Synthesis of PDMAEMA$_{64}$. CPBD (20 mg, 90 µmol), DMAEMA (1.42 g, 9.0 mmol), AIBN (1.48 mg, 9.0 µmol) and anisole (1.5 mL) were put in a Schlenk flask and bubbled with nitrogen gas for 15 min before the vessel was placed in an oil bath at 70 °C. After 6 hours the reaction mixture was cooled to room temperature and exposed to air. The mixture was precipitated in hexane before freeze-drying from acetonitrile. ^{1}H-NMR: conversion = 64 %, $M_{n,NMR}$ = 10 200 g·mol^{-1}, $M_{n,SEC}$ = 7 500 g·mol^{-1}, Đ = 1.29

Synthesis of Pr-PGA$_{98}$ (protected poly(glucose acrylate)). DDMAT (9.9 mg, 27 µmol), Pr-GA (860.3 mg, 2.7 mmol), AIBN (0.8 mg, 5 µmol) and anisole (1.5 mL) were put in a Schlenk flask and bubbled with nitrogen gas for 15 min before the vessel was placed in an oil bath at 70 °C. After 3 hours the reaction mixture was cooled to room temperature and exposed to air. The mixture was precipitated in hexane before freeze-drying from acetonitrile. ^{1}H-NMR: conversion = 97 %, $M_{n,NMR}$ =

31 100 g·mol^{-1}, $M_{n,SEC}$ = 12 500 g·mol^{-1}, Đ = 1.49

Synthesis of PDMAPAA$_{36}$. DDMAT (20 mg, 55 µmol), DMAPAA (857 mg, 5.5 mmol), AIBN (0.9 mg, 5.5 µmol) and dioxane (3.75 mL) were put in a Schlenk flask and bubbled with nitrogen gas for 15 min before the vessel was placed in an oil bath at 70 °C. After 3 hours the reaction mixture was cooled to room temperature and exposed to air. The mixture was precipitated thrice from dioxane in hexane 4:1 THF before freeze-drying from acetonitrile. ^{1}H-NMR: conversion = 36 %, $M_{n,NMR}$ = 6000 g·mol^{-1}, $M_{n,SEC}$ = 2 700 g·mol^{-1}, Đ = 1.82

Synthesis of P*t*BA$_{92}$. DDMAT (20 mg, 55 µmol), *t*BA (703 mg, 5.5 mmol), AIBN (0.9 mg, 5.5 µmol) and dioxane (3.75 mL) were put in a Schlenk flask and bubbled with nitrogen gas for 15 min before the vessel was placed in an oil bath at 80 °C. After 3 hours the reaction mixture was cooled to room temperature and exposed to air. The mixture was precipitated in hexane before freeze-drying from acetonitrile. ^{1}H-NMR: conversion = 91 %, $M_{n,NMR}$ = 12 100 g·mol^{-1}, $M_{n,SEC}$ = 7 600 g·mol^{-1}, Đ = 1.26

2.3.3 Block copolymers

Synthesis of Pr-PGMA$_{89}$-*b*-P*t*BMA$_{75}$. Pr-PGMA$_{89}$ (macro-CTA, 100 mg, 3.4 µmol), *t*BMA (48.1 mg, 0.34 mmol), AIBN (0.06 mg, 0.3 µmol) and anisole (0.29 mL) were put in a Schlenk flask and bubbled with nitrogen gas for 15 min before the vessel was placed in an oil bath at 80 °C. After 4 hours the reaction mixture was cooled to room temperature and exposed to air. The mixture was precipitated in hexane before freeze-drying from acetonitrile. ^{1}H-NMR: conversion = 72 %, $M_{n,NMR}$ = 40 500 g·mol^{-1}, $M_{n,SEC}$ = 23 700 g·mol^{-1}, Đ = 1.27

Synthesis of Pr-PGMA$_{89}$-*b*-PDMAEMA. Pr-PGMA$_{89}$ (macro-CTA, 100 mg, 3.4 µmol), DMAEMA (53.2 mg, 0.34 mmol), AIBN (0.06 mg, 0.3 µmol) and anisole (0.59 mL) were put in a Schlenk flask and bubbled with nitrogen gas for 15 min before the vessel was placed in an oil bath at 80 °C. After 4 hours the reaction mixture was cooled to room temperature and exposed to air. No conversion was observed with ^{1}H-NMR. The mixture colour changed from pink to bright orange.

Synthesis of Pr-PGA$_{98}$-*b*-P*t*BA$_{37}$. Pr-PGA$_{98}$ (macro-CTA, 100.2 mg, 3.2 µmol), *t*BA (75.1 mg, 0.59 mmol), AIBN (0.05 mg, 0.3 µmol) and anisole (1.1 mL) were put in a Schlenk flask and bubbled with nitrogen gas for 15 min before the vessel was placed in an oil bath at 70 °C. After 4 hours the reaction mixture was cooled to room temperature and exposed to air. The mixture was precipitated in hexane before freeze-drying from acetonitrile. ^{1}H-NMR: conversion = 21 %, $M_{n,NMR}$ = 36 300 g·mol^{-1}, $M_{n,SEC}$

= 15 900 g·mol^{-1}, Đ = 1.28

Synthesis of Pr-PGA$_{98}$-*b*-PDMAPAA$_{44}$. Pr-PGA$_{98}$ (macro-CTA, 99.9 mg, 3.2 µmol), DMAPAA (107.1 mg, 0.69 mmol), AIBN (0.1 mg, 0.6 µmol) and anisole (1.1 mL) were put in a Schlenk flask and bubbled with nitrogen gas for 15 min before the vessel was placed in an oil bath at 80 °C. After 22.5 hours the reaction mixture was cooled to room temperature and exposed to air. The mixture was precipitated in hexane before freeze-drying from acetonitrile. ^{1}H-NMR: conversion = 21 %, $M_{n,NMR}$ = 38 400 g·mol^{-1}, $M_{n,SEC}$ = 13 900 g·mol^{-1}, Đ = 1.59

2.3.4 Polymer modifications

Synthesis of PDMAPAA-Q$_{36}$ (quaternised PDMAPAA). PDMAPAA$_{36}$ (77.5 mg, 0.5 mmol of DMAPAA), iodomethane (155 µL, 2.5 mmol) and deionised water (10 mL) were put in a glass vessel and stirred at room temperature for 16 hours. The mixture was then bubbled with nitrogen gas for 4 hours to remove an excess of reagent before freeze-drying.

Synthesis of PAA$_{92}$. P*t*BA$_{92}$ (100 mg, 8.2 µmol), trifluoroacetic acid (9 mL) and deionised water (1 mL) were put in a glass vessel and stirred at room temperature for 3 hours. The polymer was dialysed against DI water and freeze-dried.

Synthesis of PAA$_{92}$. P*t*BA$_{92}$ (100 mg, 8.2 µmol), hexafluoroisopropanol (8 mL) and hydrochloric acid (65 µL) were put in a glass vessel and stirred at room temperature for 4 hours. The polymer was dialysed against DI water and freeze-dried.

Synthesis of PGA$_{98}$. Pr-PGA$_{98}$ (100 mg, 5 µmol), trifluoroacetic acid (9 mL) and deionised water (1 mL) were put in a glass vessel and stirred at room temperature for 3 hours. The polymer was dialysed against DI water and freeze-dried.

Synthesis of PGA$_{98}$. Pr-PGA$_{98}$ (100 mg, 5 µmol), hexafluoroisopropanol (13 mL) and hydrochloric acid (0.1 mL) were put in a glass vessel and stirred at room temperature for 4 hours. The polymer was dialysed against DI water and freeze-dried.

Synthesis of PGA$_{98}$-*b*-PAA$_{37}$. Pr-PGA$_{98}$-*b*-P*t*BA$_{37}$ (40.8 mg, 1.1 µmol), trifluoroacetic acid (9 mL) and deionised water (1 mL) were put in a glass vessel and stirred at room temperature for 3 hours. The polymer was dialysed against DI water and freeze-dried.

Synthesis of PGA_{98}-*b*-$PDMAPAA_{44}$. Pr-PGA_{98}-*b*-$PDMAPAA_{44}$ (33.9 mg, 0.9 µmol), trifluoroacetic acid (9 mL) and deionised water (1 mL) were put in a glass vessel and stirred at room temperature for 3 hours. The polymer was dialysed against DI water and freeze-dried.

Synthesis of PGA_{98}-*b*-$PDMAPAA\text{-}Q_{44}$. PGA_{98}-*b*-$PDMAPAA_{44}$ (15.4 mg, 0.5 µmol), iodomethane (100 µL, 1.6 mmol) and deionised water (10 mL) were put in a glass vessel and stirred at room temperature for 16 hours. The mixture was then bubbled with nitrogen gas for 4 hours to remove an excess of reagent before freeze-drying.

Complexation of PGA_{98}-*b*-PAA_{37} and PGA_{98}-*b*-$PDMAPAA\text{-}Q_{44}$. Samples were dissolved in a phosphate buffer at a concentration of 1 $g \cdot L^{-1}$ and filtered with a 0.45 µm filter (Whatman, cellulose acetate). The phosphate buffer was made by dissolving $Na_2HPO_4 \cdot 7H_2O$ (0.133 g, 0.5 mmol) and NaCl (0.322 g, 5.5 mmol) in Milli-Q water (50 mL). NaOH pellets and HCl droplets were then added to adjust the pH to 12. The buffer was filtered three times with 0.45 µm filters and three times with 0.2 µm filters (Whatman, cellulose acetate). Charge-stoichiometric amounts of the copolymers were mixed and put into a small glass vial. For every unit of volume of PGA_{98}-*b*-PAA_{37}, 1.18 equivalents PGA_{98}-*b*-$PDMAPAA\text{-}Q_{44}$ was added.

3 RESULTS AND DISCUSSION

In this chapter the experimental results are reported and discussed, starting with the synthesis and characterisation of monomers, polymers and modified polymers. Finally, the self-assembly of these polymers is described.

3.1 Synthesis of glycomonomers

The first step of the project was to produce glycomonomers from glucose using simple organic chemistry reactions. One way to do so is via the reaction of (meth)acryloyl chloride (*i.e.* an acid chloride with a pendant vinyl group) with a sugar possessing a single hydroxy group.[34] Glucose however has five hydroxy functions, which prevents the selective attachment of a vinyl group. Therefore, protective groups had first to be installed on all but one hydroxy function, following the introduction of vinyl functionalities. This protection results in a hydrophobic monomer, greatly simplifying its polymerisation, copolymerisation with other hydrophobic species, and characterisation. While unprotected glycopolymers have been synthesised, this can only be done using water or DMSO as solvent. Subsequent chain extension of these unprotected glycopolymers require the use of hydrophilic monomers in the same solvents.[33]

First, two acetonide (also known as isopropylidene) groups were installed onto D-(+)-glucose using acetone both as reagent and solvent and concentrated sulphuric acid as catalyst (see Materials and Methods section). The resulting protected sugar (Pr-G) was analysed by proton nuclear magnetic resonance spectroscopy (^{1}H-NMR, Figure 10b) to confirm its structure. Evidence for the successful synthesis of Pr-G is the appearance of the characteristic acetonide methyl peaks around 1.4 ppm (g_1-g_4) that were not present in the ^{1}H-NMR spectrum of D-(+)-glucose (Figure 10a). Another feature that stands out is the disappearance of all –OH peaks. This, however, does not provide any information about the synthesis as it is caused by hydrogen-deuterium exchange with the solvent ($CDCl_3$), completely quenching the –OH peak signal. Note that the solvent used for D-(+)-glucose is DMSO-d_6.

Carbon nuclear magnetic resonance spectroscopy (^{13}C-NMR, Figure 18b in Supporting Information, SI) was also performed and revealed the appearance of new carbon signals originating from the acetonide protective groups (g_1 and g_2, ~115 ppm; h_1-h_4, ~30 ppm) that were absent from the ^{13}C-NMR spectrum of D-(+)-glucose. Unfortunately, high-resolution mass spectrometry (HRMS) could not be performed on this intermediate.

Then, polymerisable vinyl moieties were installed onto the remaining hydroxy group of the protected glucose to produce glycomonomers. A slight excess of either acryloyl chloride or methacryloyl

chloride was used in the presence of triethylamine at a reduced temperature and the corresponding glycomonomers were obtained after work up and flash chromatography (see Materials and Methods section). ^{1}H-NMR analysis (see Figure 10c) demonstrates the successful synthesis of the acrylic glycomonomer (Pr-GA), supported by the rise of peaks belonging to the vinyl protons (i_1, ~6.5 ppm; i_2, ~5.9 ppm) and by the displacement of the –CH peak (c) adjacent to the acrylate function from ~4.5 ppm to ~5.3 ppm, due to the deshielding effect of the acrylate functionality. The methacrylic glycomonomer (Pr-GMA) was analysed with ^{1}H-NMR (see Figure 10d) and showed a similar trend: vinylic proton peaks (i_1, ~6.1 ppm; i_2, ~5.6 ppm), the –CH peak displacement (c, from ~4.5 ppm to ~5.3 ppm), but also the large $–CH_3$ peak (h, ~1.9 ppm) on the methacrylic moiety verify that the synthesis was successful.

^{13}C-NMR (Figure 18c in SI) also confirmed the structure of Pr-GA through the emergence of carbon signals belonging to the acrylate functionality (i, ~170 ppm; j, ~135 ppm; k, ~130 ppm). The methacrylate functionality introduced ^{13}C-NMR (Figure 18d in SI) carbon signals at roughly the same chemical shift (i, ~170 ppm; j, ~140 ppm; k, ~130 ppm), as well as a signal around 20 ppm corresponding with the methyl carbon (l). Interestingly, some carbons in Pr-GA produce two signals, whereas the carbons in Pr-GMA produce one signal each. The same trend can be seen when comparing ^{1}H-NMR spectra of the glycomonomers. This is likely caused by cis and trans isomers of Pr-GA, whereas for Pr-GMA perhaps the activation energy to reach the cis isomer state is too high at this temperature.

HRMS (Figure 19 in SI) was also performed on the glycomonomers. For Pr-GA-(Na^+), *i.e.* Pr-GA associated with a sodium ion, an experimental mass of 337.13 g·mol^{-1} was found against a theoretical mass of 337.13 g·mol^{-1}. For Pr-GMA-(Na^+) an experimental mass of 351.14 g·mol^{-1} was found, which was also equivalent to the theoretical mass of 351.14 g·mol^{-1}. These results confirm that the glycomonomers were successfully synthesised.

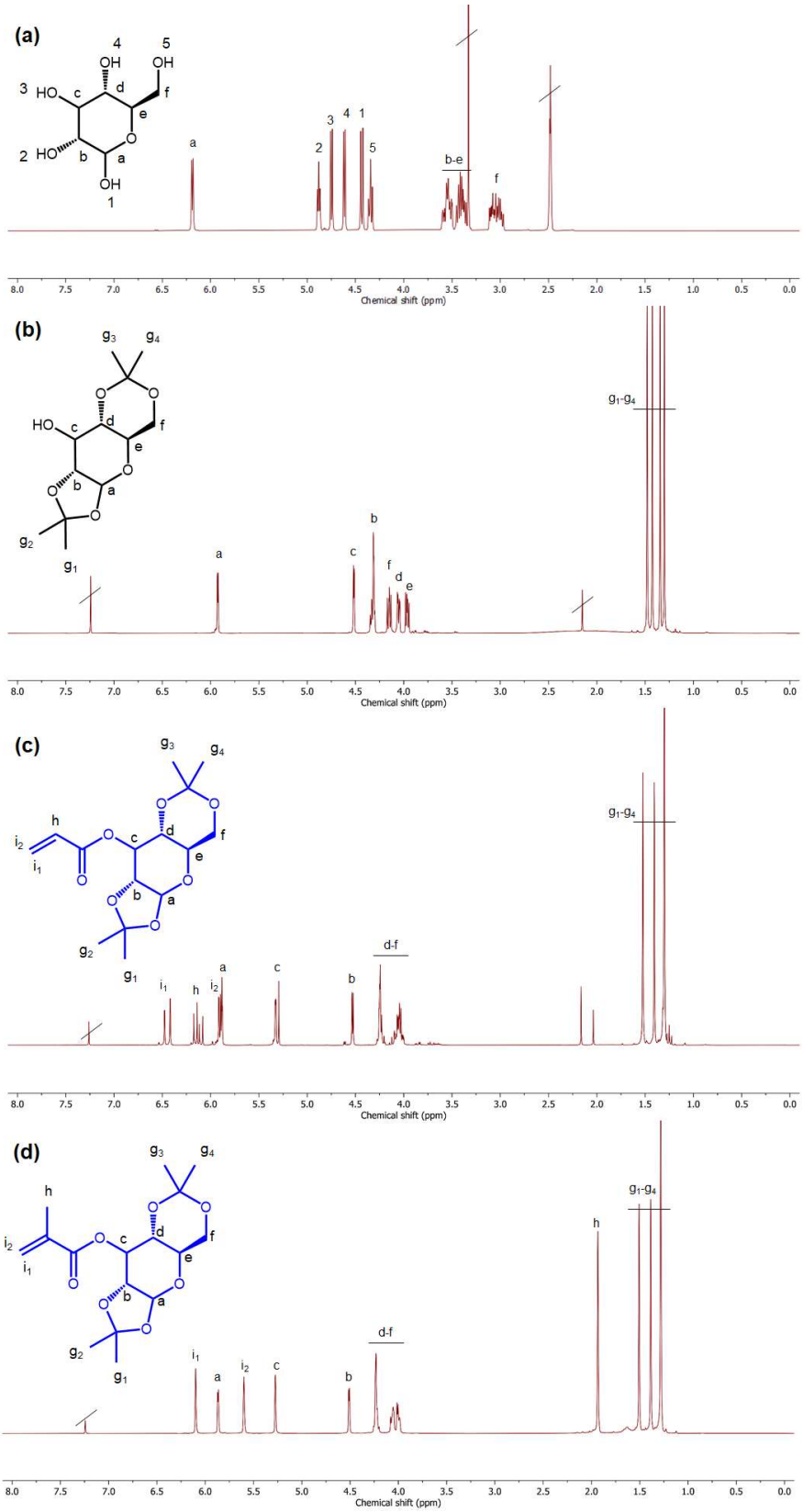

Figure 10: ^{1}H-NMR spectra of D-(+)-glucose (a, DMSO-d_6), Pr-glucose (b, $CDCl_3$), Pr-GA (c, $CDCl_3$) and Pr-GMA (d, $CDCl_3$).

3.2 Synthesis of block-type glycopolymers from dithiobenzoate RAFT agent

After synthesis and thorough characterisation of the glycomonomers we sought to produce the required block-type glycopolymers via RAFT polymerisation of Pr-GMA using a dithiobenzoate chain transfer agent. This molecule is suitable for the growth of macromolecules from methacrylic monomers.[7] We used RAFT polymerisation to first produce a protected glycopolymer macroRAFT using azobisisobutyronitrile (AIBN) as radical source and anisole as solvent. ^{1}H-NMR was used to monitor the reaction conversion by comparison of the monomer vinyl signal to an internal standard (*i.e.* anisole aromatic signal at 6.9 ppm), calculate the length and molecular weight of the polymer and verify its composition. After purification, a Pr-PGMA$_{89}$ macroRAFT (DP = 89, $M_{n,NMR}$ = 29 600 g·mol^{-1}) was obtained and its composition was confirmed by ^{1}H-NMR (Figure 11a), showing the characteristic signals corresponding with the backbone (a, ~2 ppm; b, ~1 ppm), the six-membered rings (c, ~4.8 ppm; d-f, ~4.1 ppm; h, 5.8 ppm; i, ~4.5 ppm), and the acetonide protective groups (g_1-g_4, ~1.3 ppm). Note that the characteristic signals of the polymers are typically broader than that of the respective monomers, due to the presence of similar but slightly different signals. Size-exclusion chromatography* (SEC) was performed on the Pr-PGMA$_{89}$ macroRAFT (Figure 12, $M_{n,SEC}$ = 16 900 g·mol^{-1}, Đ = 1.24). The elugram shows a relatively even distribution of molecular weights and the absence of chain-chain termination (usually evidenced by a bump at low elution time). Note that the discrepancy between M_n values obtained in ^{1}H-NMR and SEC is caused by the use of poly(methyl methacrylate) standards for the construction of an SEC calibration curve, which differ in hydrodynamic volume from the polymers synthesised during this project. Additionally, even when protected, the polar hydroxy groups present in glycopolymers can interact with the SEC column material, further distorting the $M_{n,SEC}$ values.[35]

Then, we used the protected glycopolymer with the chain transfer agent still attached on for chain extension with two different monomers to achieve block-type glycopolymers. First, *tert*-butyl methacrylate (*t*BMA) was reacted with the glycopolymer in presence of AIBN and in anisole to yield after purification protected poly(glucose methacrylate)-*block*-poly(*tert*-butyl methacrylate) (Pr-PGMA$_{89}$-*b*-P*t*BMA$_{75}$). Once more, ^{1}H-NMR was used to calculate the degree of conversion and therefore the length (DP = 75) and molecular weight ($M_{n,NMR}$ = 40 500 g·mol^{-1}). Analysis of the purified polymer (see Figure 11b) revealed a new proton signal at 1.35 ppm, characteristic for the *tert*-butyl protective groups. The SEC elugram of the block copolymer (Figure 12, $M_{n,SEC}$ = 23 700 g·mol^{-1}, Đ = 1.27) shows a homogeneous displacement of the polymer peak and a relatively even distribution

* Size-exclusion chromatography is a technique that permits the determination of the average molecular weight of a polymer and to verify the homogeneity of chain lengths and absence of chain-chain termination.

of molecular weights, indicating successful chain extension of all polymer chains and absence of chain-chain termination.

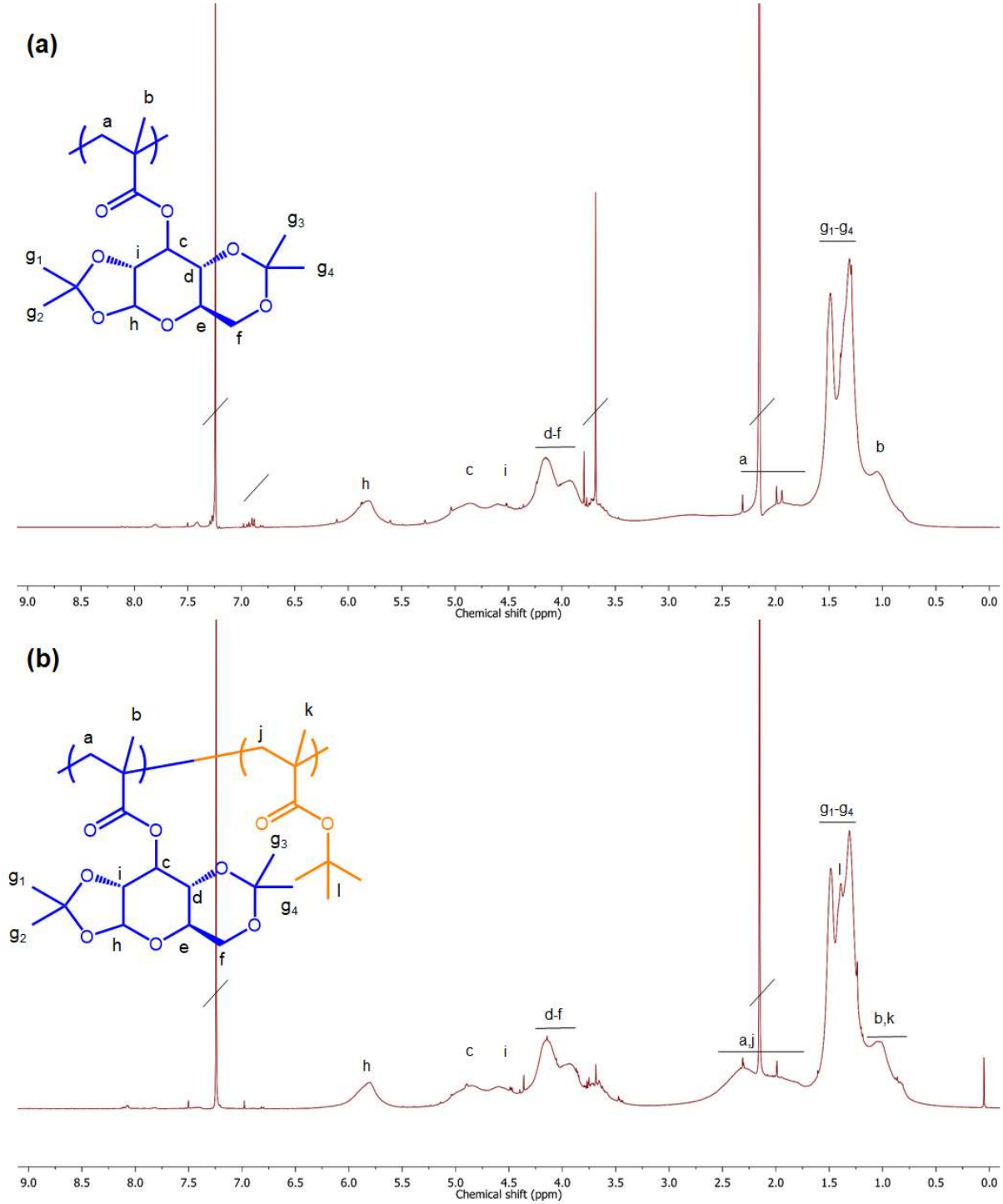

Figure 11: ^{1}H-NMR spectra of Pr-PGMA$_{89}$ (a, CDCl$_3$) and Pr-PGMA$_{89}$-b-PtBMA$_{75}$ (b, CDCl$_3$).

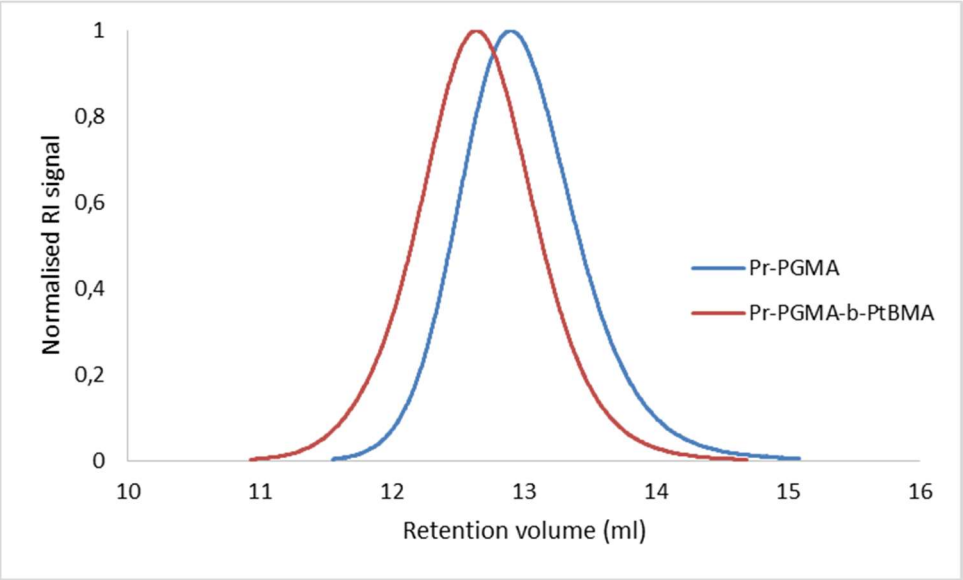

Figure 12: SEC elugrams of Pr-PGMA$_{89}$ and Pr-PGMA$_{89}$-b-PtBMA$_{75}$.

Attempts at chain extension of the same glycopolymer macroRAFT with dimethylaminoethyl methacrylate (DMAEMA) were made. The same macroRAFT was used to produce another block copolymer with equivalent chain lengths to promote self-assembly later on. Unfortunately, several reactions failed to produce the desired polymer, due to the degradation of the RAFT agent evidenced by a change of colour of the reaction mixture, from the typical pink to orange. This can be attributed to the presence of primary amine impurities in the monomer that typically cause aminolysis of the dithiobenzoate.[7] To verify that the DMAEMA monomer was the cause of the RAFT agent death, attempts were made to produce poly(dimethylaminoethyl methacrylate) (PDMAEMA) homopolymers. Within a few minutes, the reaction mixture changed colour from pink to orange and no conversion was monitored by ^{1}H-NMR. Unfortunately, switching to a new monomer bottle and vacuum distillation were not sufficient to alleviate the problems. It is possible that the monomer and the primary amine impurities form an azeotropic mixture, preventing further purification through distillation. It was therefore decided to change the synthesis route to using acrylic monomers and a more robust trithiocarbonate chain transfer agent.

In short, attempts were made to chain extend a glycopolymer macroRAFT with two monomers, individually. While chain extension with *t*BMA was successful, chain extension with DMAEMA was not. The values related to these polymers are summarised in Table 1.

Table 1: Values related to methacrylic (block-type) glycopolymers. The degree of polymerisation (DP) and molecular weight ($M_{n,NMR}$) were calculated from ^{1}H-NMR using conversion data. The molecular weight ($M_{n,SEC}$) and dispersity (Đ) were obtained by SEC using a PMMA standard series and conventional calibration curve.

Polymer	DP	$M_{n,NMR}$ (g·mol^{-1})	$M_{n,SEC}$ (g·mol^{-1})	Đ
Pr-PGMA$_{89}$	89	29 600	16 900	1.24
Pr-PGMA$_{89}$-*b*-P*t*BMA$_{75}$	75	40 500	23 700	1.27
Pr-PGMA$_{89}$-*b*-PDMAEMA	-	-	-	-

3.3 Synthesis of block-type glycopolymers from trithiocarbonate RAFT agent

After the initial setback we chose to synthesise the block-type glycopolymers using a trithiocarbonate chain transfer agent instead of the dithiobenzoate. This required a change of monomers as well: from methacrylic to acrylic (glyco)monomers, since the trithiocarbonate RAFT agent is less suitable for methacrylic monomers, but highly so for acrylates and acrylamides. We restarted by making the acrylic counterpart of the protected glycopolymer macroRAFT agent using AIBN as radical source and anisole as solvent. After purification, a Pr-PGA$_{98}$ macroRAFT (DP = 98, $M_{n,NMR}$ = 31 100 g·mol^{-1}) was obtained and its structure was verified with ^{1}H-NMR (Figure 13a), showing the characteristic signals corresponding with the backbone (a-b, ~2 ppm), the six-membered rings (c, ~5.3 ppm; d-f, ~4.2 ppm; h, 5.9 ppm; i, ~4.5 ppm), and the acetonide protective groups (g_1-g_4, ~1.3 ppm). SEC was performed on the Pr-PGA$_{98}$ macroRAFT (Figure 15, $M_{n,SEC}$ = 12 500 g·mol^{-1}, Đ = 1.49). The elugram shows a relatively even distribution of molecular weights and the absence of chain-chain termination.

Then, the glycopolymer macroRAFT was chain extended with two different monomers to produce block-type glycopolymers. Although some impurities (anisole, 1,4-dioxane and acetonitrile) remained after purification of the macroRAFT, these were not thought to inhibit sequential polymerisation. First, the glycopolymer was reacted with *tert*-butyl acrylate (*t*BA) in anisole using AIBN as radical initiator to yield protected poly(glucose acrylate)-*block*-poly(*tert*-butyl acrylate) (Pr-PGA$_{98}$-*b*-P*t*BA$_{37}$). ^{1}H-NMR analysis of the purified polymer (Figure 13b, DP = 37, $M_{n,NMR}$ = 36 300 g·mol^{-1}) revealed a new proton signal around 1.35 ppm, belonging to the *tert*-butyl protective groups. The SEC elugram of the block copolymer (Figure 15, $M_{n,SEC}$ = 15 900 g·mol^{-1}, Đ = 1.28) shows absence of chain-chain termination and homogeneous displacement of the polymer peak, which indicates successful chain extension of all polymer chains.

In order to obtain a copolymer composed of a hydrophilic glycopolymer block and a poly(acrylic acid) (PAA) block that is negatively charged above a certain pH, two deprotection reactions were necessary: the removal of acetonide groups from the Pr-PGA block and the removal of *tert*-butyl

groups from the P*t*BA block. Trifluoroacetic acid (TFA) is typically used to deprotect P*t*BA and P*t*BMA, but using hexafluoroisopropanol/hydrochloric acid (HFIP/HCl) has been shown to be far more efficient.[36] However, protected glycopolymers are commonly deprotected in TFA[37], so both methods were tested for the deprotection of P*t*BA$_{92}$ and Pr-PGA$_{98}$ and ^{1}H-NMR spectra were taken of the purified products (Figure 20 in SI). Deprotection entailed dissolving a polymer in either TFA:water (9:1 volume ratio) and stirring for three hours, or in HFIP:HCl (326:1 volume ratio) and stirring for four hours. For PAA$_{92}$ obtained with deprotection with TFA it can be seen that the peak at 1.35 ppm belonging to the *tert*-butyl groups is completely gone, whereas this peak can be observed for PAA$_{92}$ (HFIP). This is oddly contrary to what is reported in literature, but could be due to different reaction conditions. For PGA$_{98}$ (HFIP) the peak at 1.4 ppm belonging to the acetonide protective groups is completely gone, while for PGA$_{98}$ (TFA) there is a very weak signal. Overall, the PGA$_{98}$ (TFA) spectrum shows far fewer impurities than PGA$_{98}$ (HFIP). It was ultimately decided to do both deprotection reactions at once in TFA, because this method has been successfully demonstrated in literature for the deprotection of glycopolymers.[37]

The copolymer was dissolved in TFA:water in a 9:1 volume ratio and stirred for three hours, to remove the acetonide and *tert*-butyl protective groups from the repeating units, producing poly(glucose acrylate)-*block*-poly(acrylic acid) (PGA$_{98}$-*b*-PAA$_{37}$) after purification by extensive dialysis against water. In the ^{1}H-NMR spectrum (Figure 13c) it can be seen that the peaks from both the *tert*-butyl and acetonide protective groups around 1.4 ppm have largely disappeared, indicating a successful deprotection.

For the second block-type glycopolymer, the same macroRAFT was chain extended with dimethylaminopropyl acrylamide (DMAPAA) using AIBN as radical source and anisole as solvent, yielding protected poly(glucose acrylate)-*block*-poly(dimethylaminopropyl acrylamide) (Pr-PGA$_{98}$-*b*-PDMAPAA$_{44}$). This copolymer was subsequently purified and analysed with ^{1}H-NMR (Figure 14a) to obtain its chain length (DP = 44), molecular weight ($M_{n,NMR}$ = 38 400 g·mol^{-1}), and to confirm its structure. Proof of synthesis is provided by the –NH peak (o, ~7.8 ppm), the adjacent –CH_2 peaks (k, ~3.2 ppm; l, ~1.7 ppm; m, ~2.3 ppm), and the –$N(CH_3)_2$ peak (n, ~2.3 ppm). SEC was performed on the block copolymer (Figure 15, $M_{n,SEC}$ = 13 900 g·mol^{-1}, Đ = 1.59) showing a mostly homogeneous displacement of the polymer peak, which indicates successful chain extension of most polymer chains. A bit of tailing can be seen in the elugram, however, likely corresponding with the relatively high Đ.

Much like the other block copolymer, a deprotection reaction was needed to remove the acetonide groups from the Pr-PGA block, followed by a second reaction: quaternisation of the PDMAPAA block.

This deprotection reaction was performed using TFA to obtain poly(glucose acrylate)-*block*-poly(dimethylaminopropyl acrylamide) (PGA_{98}-*b*-$PDMAPAA_{44}$). A ^{1}H-NMR spectrum of the purified product is presented in Figure 14b. A quick comparison with Figure 14a shows that the peaks of the protective groups have largely disappeared, meaning that the protective groups have mostly been removed. A second modification was needed to introduce a permanent positive charge to the repeating units of the PDMAPAA block. This was done by quaternisation of the amino moiety using iodomethane in deionised water following a reported procedure[38-39], yielding poly(glucose acrylate)-*block*-poly(quaternised dimethylaminopropyl acrylamide) (PGA_{98}-*b*-PDMAPAA-Q_{44}). Analysis with ^{1}H-NMR of the purified copolymer (Figure 14c) shows the shifting of the $-(CH_3)_3$ peak (n') to 2.93 ppm from 2.76 ppm (Figure 14b). This is typical upon quaternisation and therefore an indication thereof. Furthermore, the polymer was fully soluble in D_2O and high pH aqueous media, while the non-quaternised polymer was not.

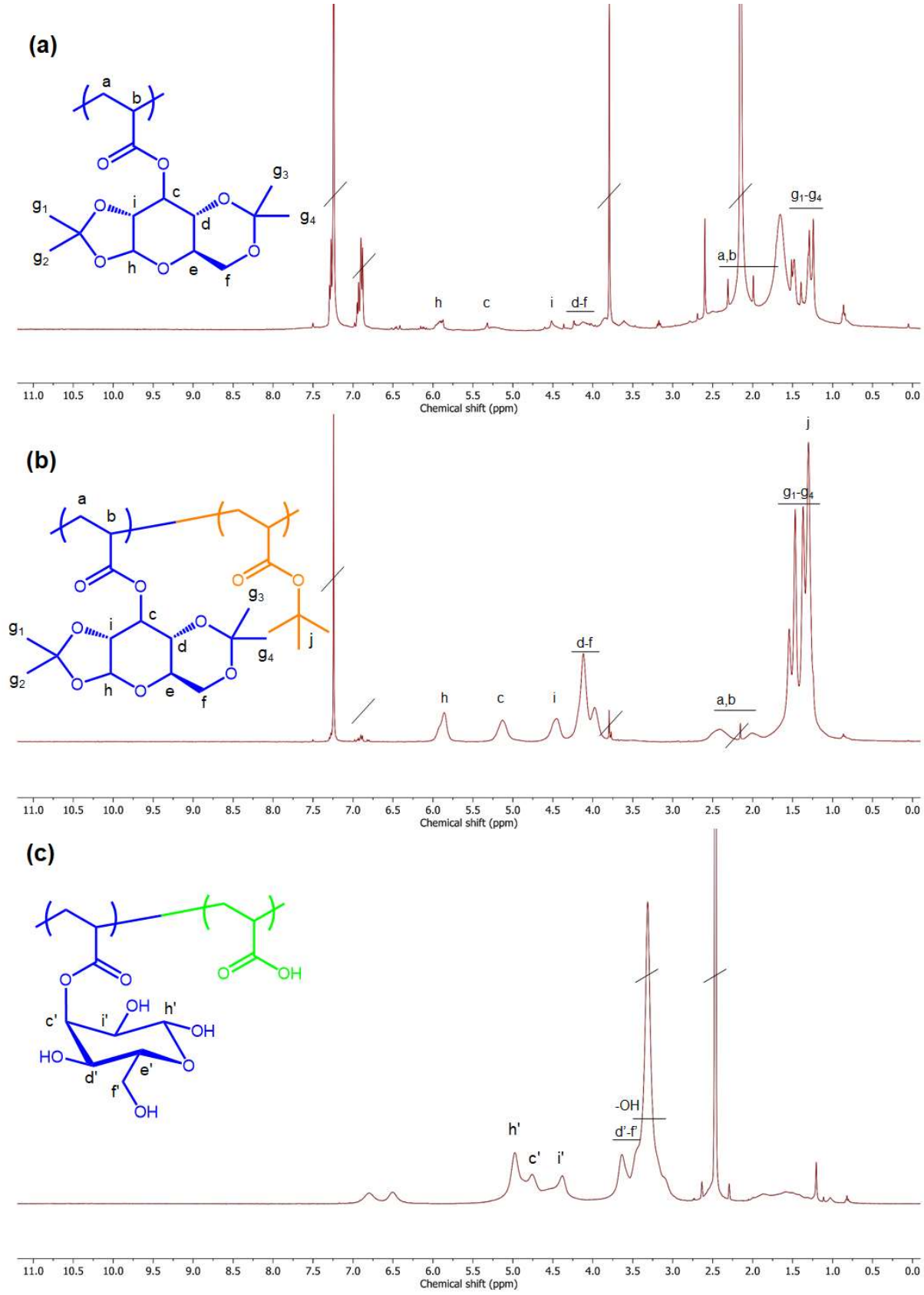

Figure 13: ^{1}H-NMR spectra of Pr-PGA$_{98}$ (a, CDCl$_3$), Pr-PGA$_{98}$-b-PtBA$_{37}$ (b, CDCl$_3$) and PGA$_{98}$-b-PAA$_{37}$ (c, DMSO-d$_6$).

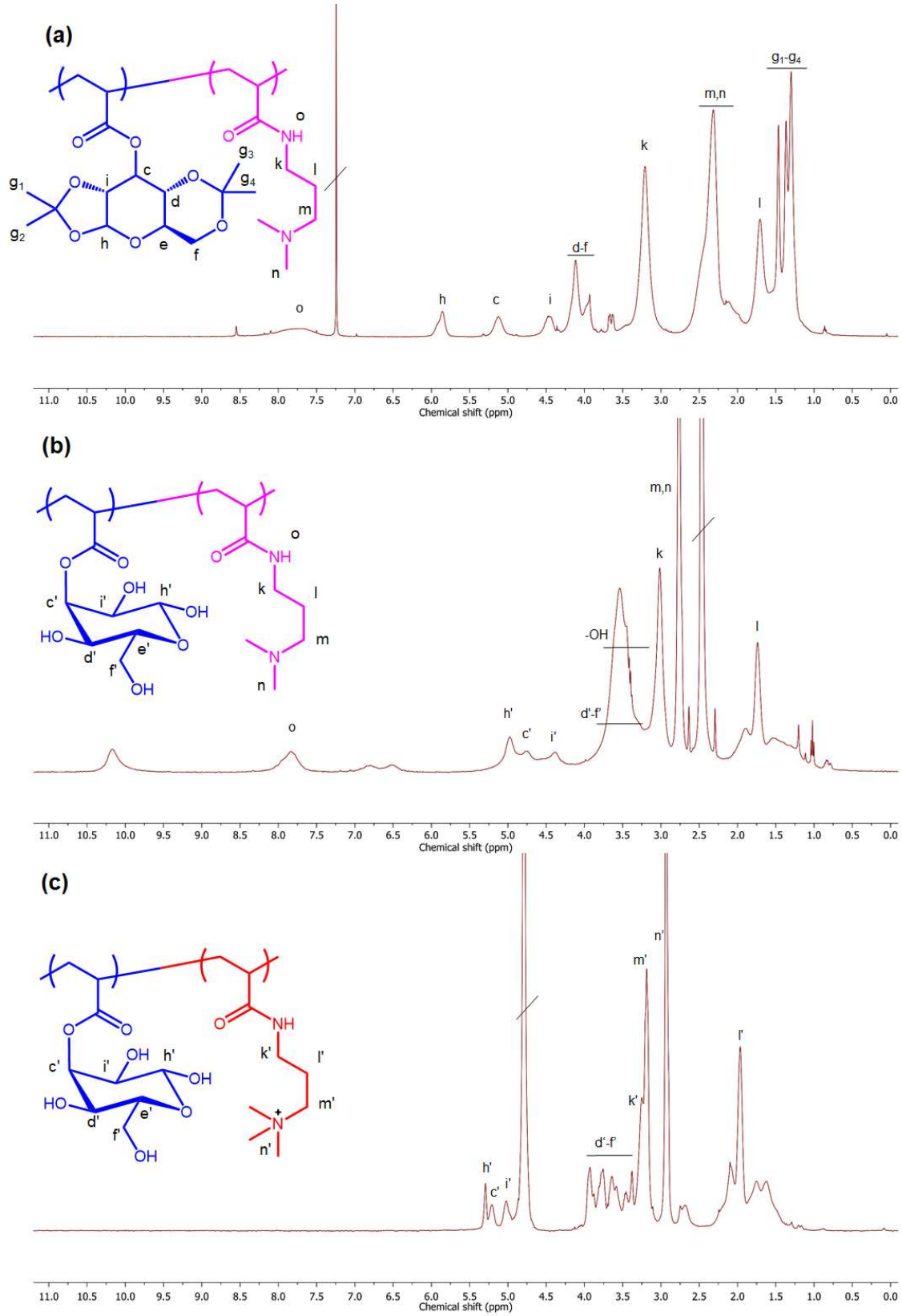

Figure 14: ^{1}H-NMR spectra of Pr-PGA$_{98}$-b-PDMAPAA$_{44}$ (a, CDCl$_3$), PGA$_{98}$-b-PDMAPAA$_{44}$ (b, DMSO-d$_6$) and PGA$_{98}$-b-PDMAPAA-Q$_{44}$ (c, D$_2$O).

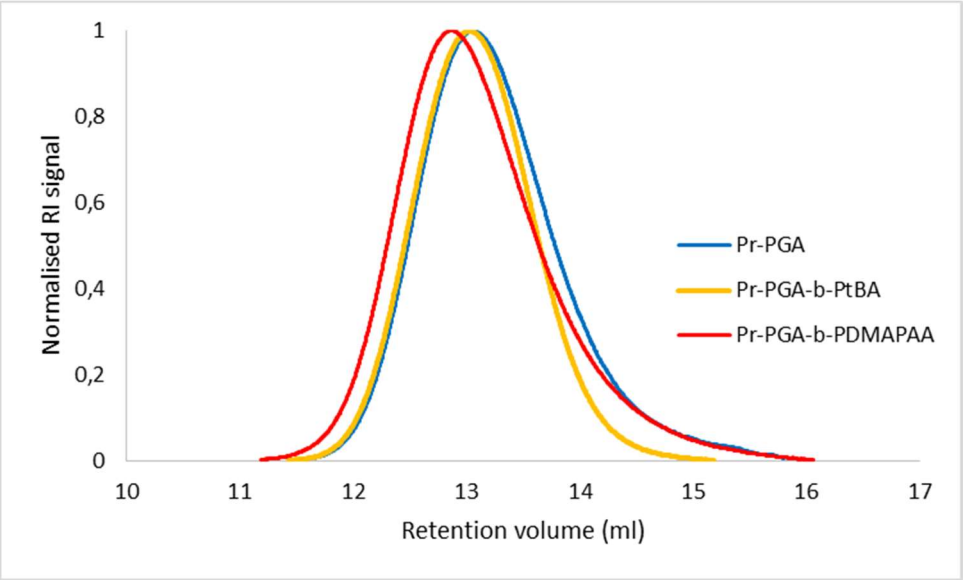

Figure 15: SEC elugrams of Pr-PGA$_{98}$, Pr-PGA$_{98}$-b-PtBA$_{37}$ and Pr-PGA$_{98}$-b-PDMAPAA$_{44}$.

To sum up, two different block-type glycopolymers were made by chain extension of a glycopolymer macroRAFT. These copolymers were subsequently modified in preparation of their self-assembly. The values related to the unmodified polymers are summarised in Table 2.

Table 2: Values related to methacrylic (block-type) glycopolymers. The degree of polymerisation (DP) and molecular weight ($M_{n,NMR}$) were calculated from ^{1}H-NMR using conversion data. The molecular weight ($M_{n,SEC}$) and dispersity (Đ) were obtained by SEC using a PMMA standard series and conventional calibration curve.

Polymer	DP	$M_{n,NMR}$ (g·mol^{-1})	$M_{n,SEC}$ (g·mol^{-1})	Đ
Pr-PGA$_{98}$	98	31 100	12 500	1.49
Pr-PGA$_{98}$-*b*-P*t*BA$_{37}$	37	36 300	15 900	1.28
Pr-PGA$_{98}$-*b*-PDMAPAA$_{44}$	44	38 400	13 900	1.59

3.4 Polymer self-assembly

Now that the block-type glycopolymers were successfully synthesised and modified, the next step was to observe whether self-assembly occurred upon mixing of the copolymers. First the glycopolymers were individually dissolved in a pH 12 phosphate buffer that was filtered to remove dust (see Materials and Methods section) at a concentration of 1 g·L^{-1}. This pH was chosen to ensure that the carboxylic acid moieties of the PAA block were deprotonated, and thus, negatively charged. Note that the quaternary ammonium cations of the PDMAPAA block are charged at any pH. Charge-

stoichiometric amounts of the polymer solutions were then mixed. Dynamic light scattering* (DLS) experiments were carried out to compare the particle sizes of the polymer solutions (Figure 16). It is clear from DLS that the mixed polymer solution (*i.e.* PGA_{98}-*b*-PAA_{37} mixed with PGA_{98}-*b*-PDMAPAA-Q_{44}) particle size is much larger than that of the individual polymer solutions. In fact, the average size of the particles in the separate solutions is comparable (PGA_{98}-*b*-PAA_{37}: 4.6 nm, PGA_{98}-*b*-PDMAPAA-Q_{44}: 5.2 nm), whereas the average particle size in the mixed solution is significantly larger: 144 nm.

ζ-potential measurements were carried out as well to quantify the magnitude of the charge on the individual block-type glycopolymers (Figures 21-23 in SI). The ζ-potential of the PGA_{98}-*b*-PAA_{37} solution was -23.7 mV, while that of the PGA_{98}-*b*-PDMAPAA-Q_{44} was -18.2 mV. These values were subtracted with the ζ-potential of the phosphate buffer (-19.1 mV), to give relative values of -4.6 mV for the negatively charged PGA_{98}-*b*-PAA_{37} and 0.9 mV for the positively charged PGA_{98}-*b*-PDMAPAA-Q_{44}. It should be noted however, that in literature it is advised not to relate the ζ-potential to charge density.[40]

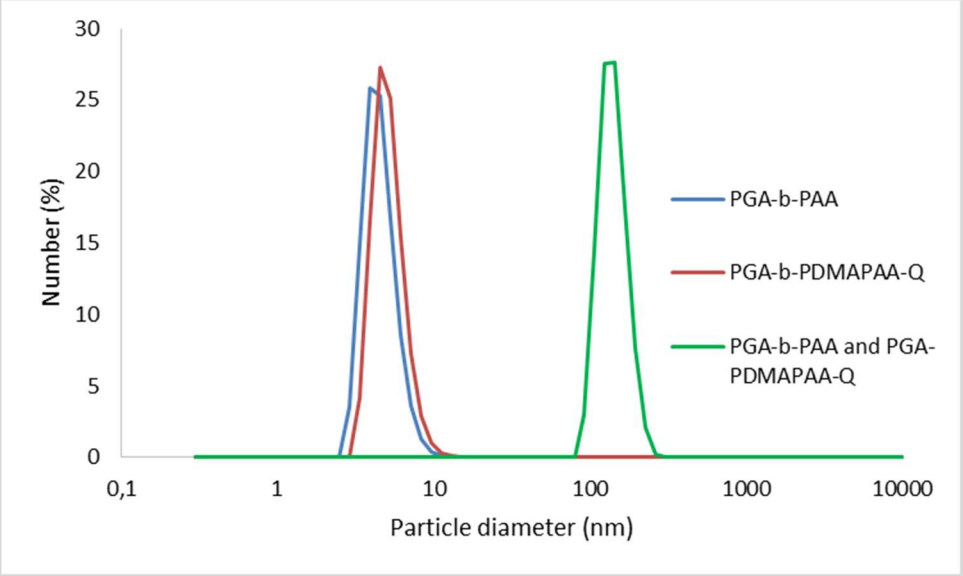

Figure 16: DLS number distribution of the glycopolymers in a pH 12 phosphate buffer at 1 g·L^{-1}.

To verify the formation of nanostructures, tapping-mode atomic force microscopy (AFM) was employed on the same polymer solution (PGA_{98}-*b*-PAA_{37} mixed with PGA_{98}-*b*-PDMAPAA-Q_{44}) that

* Dynamic light scattering is a technique used to determine the size distribution profile of, for example, polymers in solution.

was spin coated onto a freshly cleaned silicon wafer*, revealing nanoparticles of similar dimensions (height images in Figure 17, corresponding phase image in Figure 24 in SI). Due to their size and morphology, it is assumed that these particles are spherical micelles formed from the electrostatic self-assembly of the block-type glycopolymers. Cross section analysis of one nanoparticle (Figure 17c) provided its diameter (~77 nm) and height (~18 nm), while statistical analysis of 10 nanoparticles (Table 3 in SI) provided a mean diameter of 64 nm ± 6 nm, and a mean height of 16 nm ± 4 nm (the error is a 95% confidence interval). Of course, a sample size of 10 is very low, and some particles were difficult to measure due to overlap. It should also be noted that the observed particle morphology is affected by tip convolution effects, and the particles themselves are flattened in the process of sample preparation.[2] Their morphology might therefore not be representative of the nanoparticles in solution. It was observed that these particles tended to cluster into small groups, meaning that there are possibly strong favourable interactions between the particles, and/or that they physically entangle.

* A silicon wafer was chosen as substrate instead of a mica disc because silicon oxide has a much lower surface charge density than mica, which is slightly negatively charged and might have interfered with the self-assembly of the glycopolymers.[41]

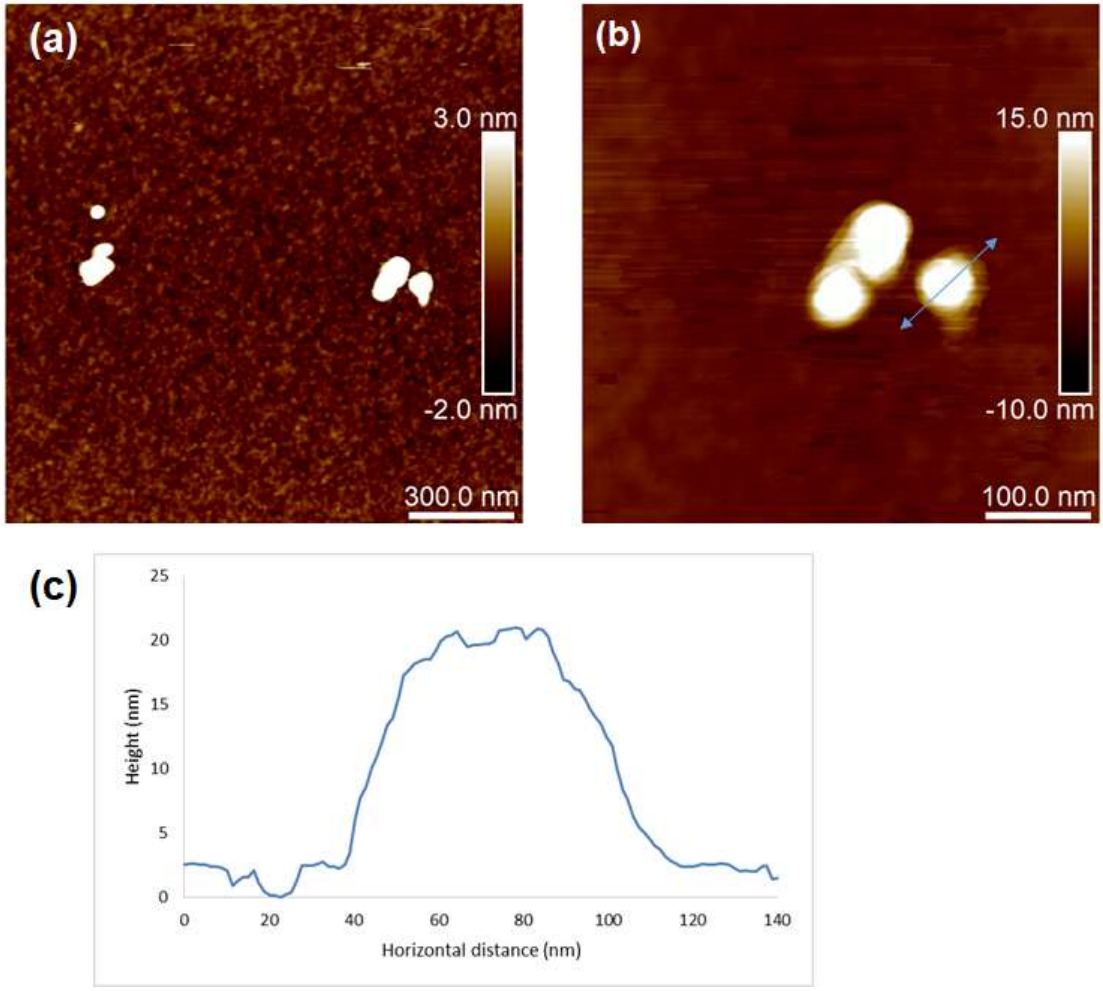

Figure 17: (a and b) AFM height images of nanoparticles formed by electrostatic complexation between PGA_{98}-b-PAA_{37} and PGA_{98}-b-PDMAPAA-Q_{44}. (c) Cross-section analysis of one nanoparticle (blue arrow).

4 CONCLUSIONS AND OUTLOOK

The goal of this master's thesis was to explore the formation of glycosylated nanoparticles through electrostatic interactions between oppositely charged block-type glycopolymers. First, a protected methacrylic glycomonomer (Pr-GMA) was synthesised by selectively attaching a methacrylate functionality onto a single hydroxy group in D-(+)-glucose. This selective reaction was made possible by first installing protective groups on all but one hydroxy function. Glycomonomer synthesis was confirmed with proton and carbon nuclear magnetic resonance spectroscopy (^{1}H-NMR and ^{13}C-NMR), and high-resolution mass spectrometry (HRMS). This glycomonomer was subsequently used to produce a glycopolymer macroRAFT (Pr-PGMA$_{89}$) via RAFT polymerisation using a dithiobenzoate chain transfer agent. All synthesised polymers were extensively characterised by ^{1}H-NMR spectroscopy and size-exclusion chromatography. Chain extension of this macroRAFT with *tert*-butyl methacrylate (*t*BMA) successfully yielded a block-type glycopolymer (Pr-PGMA$_{89}$-*b*-P*t*BMA$_{75}$), while attempts at chain extension of the macroRAFT with dimethylaminoethyl methacrylate failed, due to aminolysis of the dithiobenzoate RAFT agent caused by primary amine impurities in the monomer.

The synthesis route was therefore revised, and it was decided to use acrylic monomers and a more robust trithiocarbonate chain transfer agent. This required the synthesis of the acrylic counterpart of the glycomonomer (Pr-GA), which was then polymerised to obtain an acrylic glycopolymer macroRAFT: Pr-PGA$_{98}$. The macroRAFT was chain extended separately with two different monomers (*tert*-butyl acrylate, *t*BA, and dimethylaminopropyl acrylamide, DMAPAA) producing two block-type glycopolymers: Pr-PGA$_{98}$-*b*-P*t*BA$_{37}$ and Pr-PGA$_{98}$-*b*-PDMAPAA$_{44}$. These block copolymers were then modified with deprotection reactions, and quaternisation of the amino moieties in the PDMAPAA block, yielding PGA$_{98}$-*b*-PAA$_{37}$ and PGA$_{98}$-*b*-PDMAPAA-Q$_{44}$. Modifications were verified using ^{1}H-NMR spectroscopy.

Next, the glycopolymers were dissolved in a phosphate buffer at pH 12 to ensure that the carboxylic acid moieties on the poly(acrylic acid) (PAA) block were negatively charged. Finally, the positively charged PGA$_{98}$-*b*-PDMAPAA-Q$_{44}$ copolymer was mixed with the negatively charged PGA$_{98}$-*b*-PAA$_{37}$ copolymer, resulting in a significant increase in average particle size (observed with dynamic light scattering), and nanoparticles with a mean diameter of 64 nm ± 6 nm and mean height of 16 nm ± 4 nm (found with atomic force microscopy). These findings were ascribed to the formation of spherical micelles due to the electrostatic self-assembly of the glycopolymers, achieving the goal of this master's thesis.

This research can be expanded upon by, for example, investigating whether the self-assembled micelles are suitable for drug delivery. A start would be to determine the reversibility of the electrostatic complexation. This can be done by changing the parameters of the polymer solution (*e.g.* pH, ionic strength, or temperature).[42] It would be interesting to examine whether the micelles disintegrate at low pH (and thus, neutral PGA_{98}-*b*-PAA_{37}), which would further support the claim that their self-assembly is caused by electrostatic complexation. Once reversible aggregation of the nanoparticles has been achieved the next step would be to load them with model drugs. Some commonly used drugs for this purpose include curcumin, doxorubicin, indomethacin, fenofibrate and progesterone.[43-44] To measure the extent of drug loading, UV-Vis analysis and fluorescence studies are typically used.[27] Finally, drug delivery into, for example, isolated cancer cells could be studied.

5 REFERENCES

[1] R. Mülhaupt, Green polymer chemistry and bio-based plastics: dreams and reality, *Macromol. Chem. Phys.* **2012**, 214, 159.

[2] T. Pelras, Nanostructured soft matter from compartmentalised molecular polymer brushes (Doctoral dissertation, University of Sydney), **2019**.

[3] A. Hirao, R. Goseki and T. Ishizone, Advances in living anionic polymerization: From functional monomers, polymerization systems, to macromolecular architectures, *Macromol*. **2014**, 47, 1883.

[4] S. Aoshima and S. Kanaoka, A renaissance in living cationic polymerization, *Chem. Rev*. **2009**, 109, 5245.

[5] J. Chiefari, Y.K. Chong, F. Ercole, J. Krstina, J. Jeffery, T.P.T. Le, R.T.A Mayadunne, G.F. Meijs, C.L. Moad, G. Moad, E. Rizzardo and S.H. Thang, Living free-radical polymerization by reversible addition-fragmentation chain transfer: the RAFT process, *Macromol*. **1998**, 31, 5559.

[6] S. Perrier, 50th anniversary perspective: RAFT polymerization – A user guide, *Macromol*. **2017**, 50, 7433.

[7] H. Willcock and R.K. O'Reilly, End group removal and modification of RAFT polymers, *Polym. Chem*. **2010**, 1, 149.

[8] G. Moad, E. Rizzardo and S.H. Thang, RAFT polymerization and some of its applications, *Chem. Asian J*. **2013**, 8, 1634.

[9] S. Bas and M.D. Soucek, Synthesis, characterization and properties of amphiphilic block copolymers of 2-hydroxyethyl methacrylate and polydimethylsiloxane prepared by atom transfer radical polymerization, *Polym. J*. **2012**, 44, 1087.

[10] I.W. Hamley, Self-assembly of amphiphilic peptides, *Soft Matter*, **2011**, 7, 4122.

[11] R. Nagarajan and E. Ruckenstein, Theory of surfactant self-assembly: A predictive molecular thermodynamic approach, *Langmuir*, **1991**, 7, 2934.

[12] Y. Mai and A. Eisenberg, Self-assembly of block copolymers, *Chem. Soc. Rev*. **2012**, 41, 5969.

[13] D.V. Pergushov, A.H.E. Müller and F.H. Schacher, Micellar interpolyelectrolyte complexes, *Chem. Soc. Rev*. **2012**, 41, 6888.

[14] M. Li, W. Song, Z. Tang, S. Lv, L. Lin, H. Sun, Q. Li, Y. Yang, H. Hong and X. Chen, Nanoscaled poly(L-glutamic acid)/doxorubicin-amphiphile complex as pH-responsive drug delivery system for effective treatment of non-small cell lung cancer, *ACS Appl. Mater. Interfaces*, **2013**, 5, 1781.

[15] S.H. Kim, J.H. Jeong, S.H. Lee, S.W. Kim, T.G. Park, Local and systemic delivery of VEGF siRNA using polyelectrolyte complex micelles for effective treatment of cancer, *J. Cont. Rel.* **2008**, 129, 107.

[16] S. Katayose and K. Kataoka, Water-soluble polyion complex associates of DNA and poly(ethylene glycol)−poly(l-lysine) block copolymer, *Bioconjugate Chem*. **1997**, 8, 702.

[17] T.I. Löbling, J.S. Haataja, C.V. Synatschke, F.H. Schacher, M. Müller, A. Hanisch, A.H. Gröschel and A.H.E. Müller, Hidden structural features of multicompartment micelles revealed by cryogenic transmission electron tomography, *ACS Nano*, **2014**, 8, 11330.

[18] C.V. Synatschke, F.H. Schacher, M. Förtsch, M. Drechsler and A.H.E. Müller, Double-layered micellar interpolyelectrolyte complexes—how many shells to a core? *Soft Matter*, **2011**, 7, 1714.

[19] J. Gohy, S.K. Varshney and R. Jérôme, Water-soluble complexes formed by poly(2-vinylpyridinium)-*block*-poly(ethylene oxide) and poly(sodium methacrylate)-*block*-poly(ethylene oxide) copolymers, *Macromol*. **2001**, 34, 3361.

[20] I.K. Voets, P.M. Moll, A. Aqil, C. Jérôme, C. Detrembleur, P. de Waard, A. de Keizer and M.A. Cohen Stuart, Temperature responsive complex coacervate core micelles with a PEO and PNIPAAm corona, *J. Phys. Chem. B*, **2008**, 112, 10833.

[21] C. Dähling, G. Lotze, M. Drechsler, H. Mori, D.V. Pergushov and F.A. Plamper, Temperature-induced structure switch in thermo-responsive micellar interpolyelectrolyte complexes: toward core-shell-corona and worm-like morphologies, *Soft Matter*, **2016**, 12, 5127.

[22] C. Dähling, J.E. Houston, A. Radulescu, M. Drechsler, M. Brugnoni, H. Mori, D.V. Pergushov and F.A. Plamper, Self-templated generation of triggerable and restorable nonequilibrium micelles, *ACS Macro Lett*. **2018**, 7, 341.

[23] I. Insua, A. Wilkinson and F. Fernandez-Trillo, Polyion complex (PIC) particles: Preparation and biomedical applications, *Eur. Polym. J*. **2016**, 81, 198.

[24] O. León, A. Muñoz-Bonilla, V. Bordegé, M. Sánchez-Chaves and M. Fernández-García, Amphiphilic block glycopolymers via atom transfer radical polymerization: synthesis, self-assembly and biomolecular recognition, *J. Polym. Sci. A Polym. Chem*. **2011**, 49, 2627.

[25] A.S. Volokhova, K.J. Edgar and J.B. Matson, Polysaccharide-containing block copolymers: synthesis and applications, *Mater. Chem. Front.* **2020**, 4, 99.

[26] T. Pelras and K. Loos, Strategies for the synthesis of sequence-controlled glycopolymers and their potential for advanced applications, **2020**.

[27] C. Cao, J. Zhao, F. Chen, M. Lu, Y.Y. Khine, A. Macmillan, C.J. Garvey and M.H. Stenzel, Drug-induced morphology transition of self-assembled glycopolymers: Insight into the drug-polymer interaction, *Chem. Mater*. **2018**, 30, 5227.

[28] Y. Wang, Y. Kotsuchibashi, Y. Liu and R. Narain, Study of bacterial adhesion on biomimetic temperature responsive glycopolymer surfaces, *ACS Appl. Mater. Interfaces*, **2015**, 7, 1652.

[29] A. Muñoz-Bonilla, O. León, M.L. Cerrada, J. Rodríguez-Hernández, M. Sánchez-Chaves and M. Fernández-García, Chemical modification of block copolymers based on 2-hydroxyethyl acrylate to obtain amphiphilic glycopolymers, *Eur. Polym. J*. **2015**, 62, 167.

[30] K. Chen, M. Bao, A. Muñoz-Bonilla, W. Zhang and G. Chen, A biomimicking and electrostatic self-assembly strategy for the preparation of glycopolymer decorated photoactive nanoparticles, *Polym. Chem.* **2016**, 7, 2565.

[31] T. Pelras, J. Benninga and K. Loos, Electrostatic complexation between glucose-based block copolymers, **2020**, Poster presented at the CHemistry As INnovative Science (CHAINS) conference.

[32] T. Pelras, Nonappa, C.S. Mahon and M. Müllner, Cylindrical zwitterionic particles via interpolyelectrolyte complexation on molecular polymer brushes, *Macromol. Rapid Commun.* **2020**, 2000401.

[33] A. Adharis, T. Ketelaar, A.G. Komarudin and K. Loos, Synthesis and self-assembly of double-hydrophilic and amphiphilic block glycopolymers, *Biomacromol.* **2019**, 20, 1325.

[34] L. Albertin, M. Stenzel, C. Barner-Kowollik, L.J.R. Foster and T.P Davis, Well-defined glycopolymers from RAFT polymerization: Poly(methyl 6-*O*-methacryloyl-α-$_D$-glucoside) and its block copolymer with 2-hydroxyethyl methacrylate, *Macromol.* **2004**, 37, 7530.

[35] G. Nagy, T. Peng and N.L.B. Pohl, Recent liquid chromatographic approaches and developments for the separation of carbohydrates, *Anal. Methods*, **2017**, 9, 3579.

[36] A. D. Filippov, I.A. van Hees, R. Fokkink, I.K. Voets and M. Kamperman, Rapid and quantitative de-*tert*-butylation for poly(acrylic acid) block copolymers and influence on relaxation of thermoassociated transient networks, *Macromol.* **2018**, 51, 8316.

[37] C. Boyer, A. Bousquet, J. Rondolo, M.R. Whittaker, M.H. Stenzel and T.P Davis, Glycopolymer decoration of gold nanoparticles using a LbL approach, *Macromol.* **2010**, 43, 3775.

[38] T. Pelras, C.S. Mahon, Nonappa, O. Ikkala, A.H. Gröschel and M. Müllner, Polymer nanowires with highly precise internal morphology and topography, *J. Am. Chem. Soc.* **2018**, 140, 12736.

[39] M. Müllner, T. Lunkenbein, J. Breu, F. Caruso and A.H.E. Müller, Template-directed synthesis of silica nanowires and nanotubes from cylindrical core-shell polymer brushes, *Chem. Mater.* **2012**, 24, 1802.

[40] S. Bhattacharjee, DLS and zeta potential – What they are and what they are not? *J. Cont. Rel.* **2016**, 235, 337.

[41] M.A. Pillers, R. Schute, A. Farchone, K.P. Linder, R. Doerfler, C. Gavin, V. Goss, M. Lieberman, Preparation of mica and silicon substrates for DNA origami analysis and experimentation, *J. Vis. Exp.* **2015**, 101.

[42] C.C.M. Sproncken, J.R. Magana and I.K. Voets, 100th Anniversary of macromolecular science viewpoint: Attractive soft matter: Association kinetics, dynamics, and pathway complexity in electrostatically coassembled micelles, *ACS Macro Lett.* **2021**, 10, 167.

[43] W. Stuart-Walker and C.S. Mahon, Glycomacromolecules: Addressing challenges in drug delivery and therapeutic development, *Adv. Drug Deliv. Rev.* **2021**, 171, 77.

[44] V.P. Sant, D. Smith and J. Leroux, Novel pH-sensitive supramolecular assemblies for oral delivery of poorly water soluble drugs: preparation and characterization, *J. Cont. Rel.* **2004**, 97, 301.

6 SUPPORTING INFORMATION

6.1 ^{13}C-NMR spectra of glycomonomer synthesis

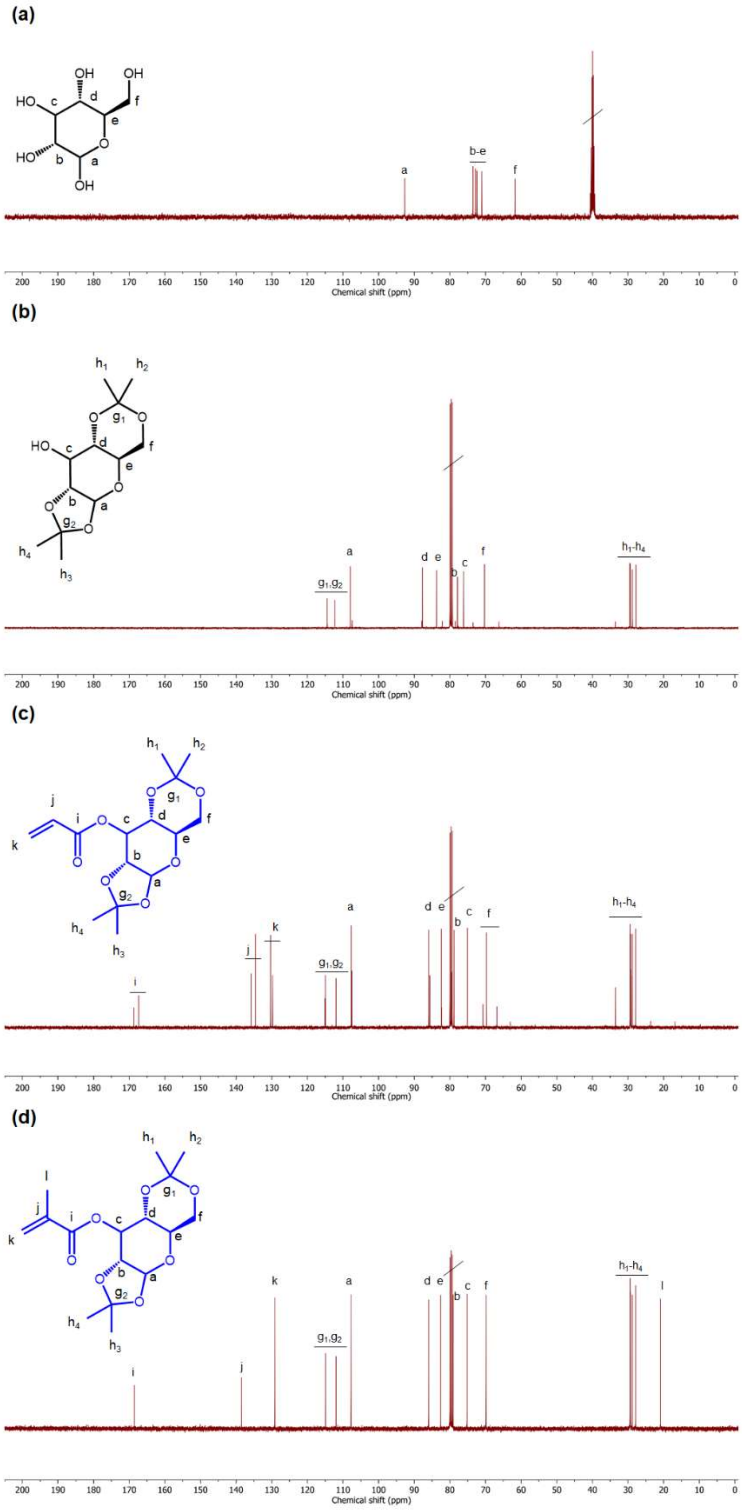

Figure 18: a) ^{13}C-NMR spectra of D-(+)-glucose (a, DMSO-d_6), Pr-glucose (b, $CDCl_3$), Pr-GA (c, $CDCl_3$) and Pr-GMA (d, $CDCl_3$).

6.2 HRMS spectra of glycomonomers

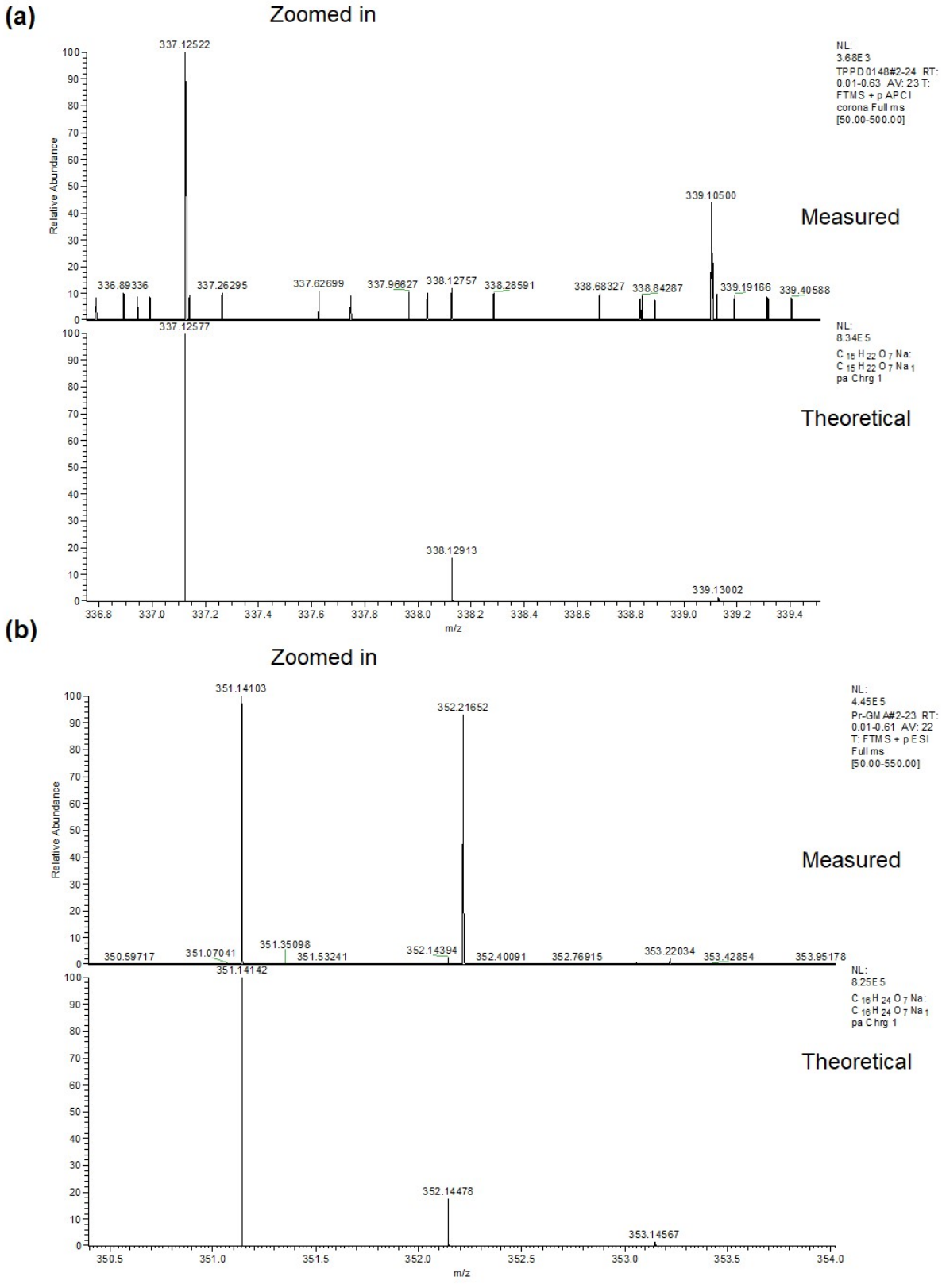

Figure 19: HRMS spectra of (a) Pr-GA and (b) Pr-GMA.

6.3 ^{1}H-NMR spectra of the deprotection of P*t*BA and Pr-PGA with TFA or HFIP

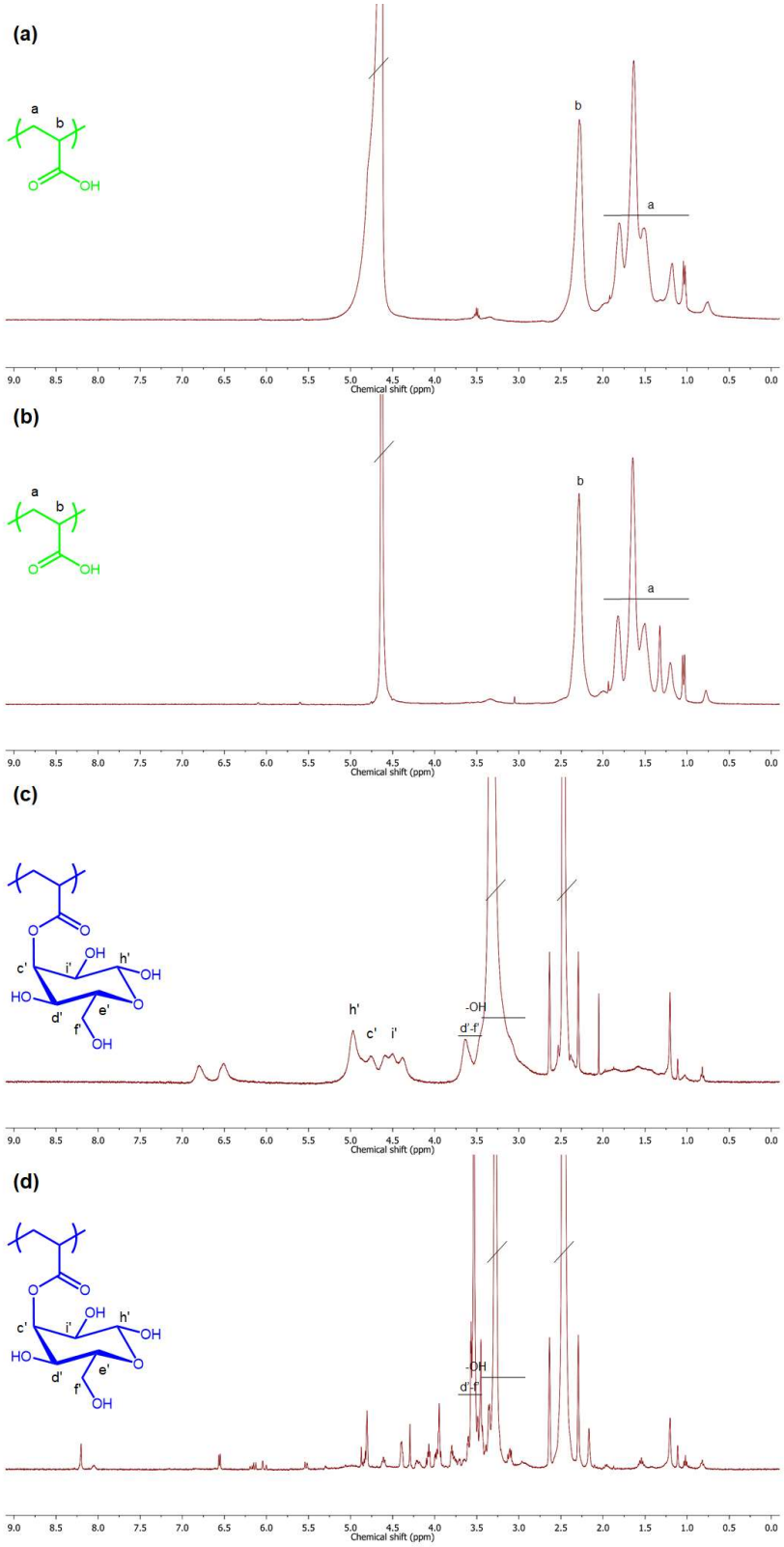

Figure 20: ^{1}H-NMR spectra of PAA (a, TFA, D_2O), PAA (b, HFIP, D_2O), PGA (c, TFA, DMSO-d_6) and PGA (d, HFIP, DMSO-d_6).

6.4 ζ-potential measurements

Figure 21: ζ-potential measurement of the pH 12 phosphate buffer.

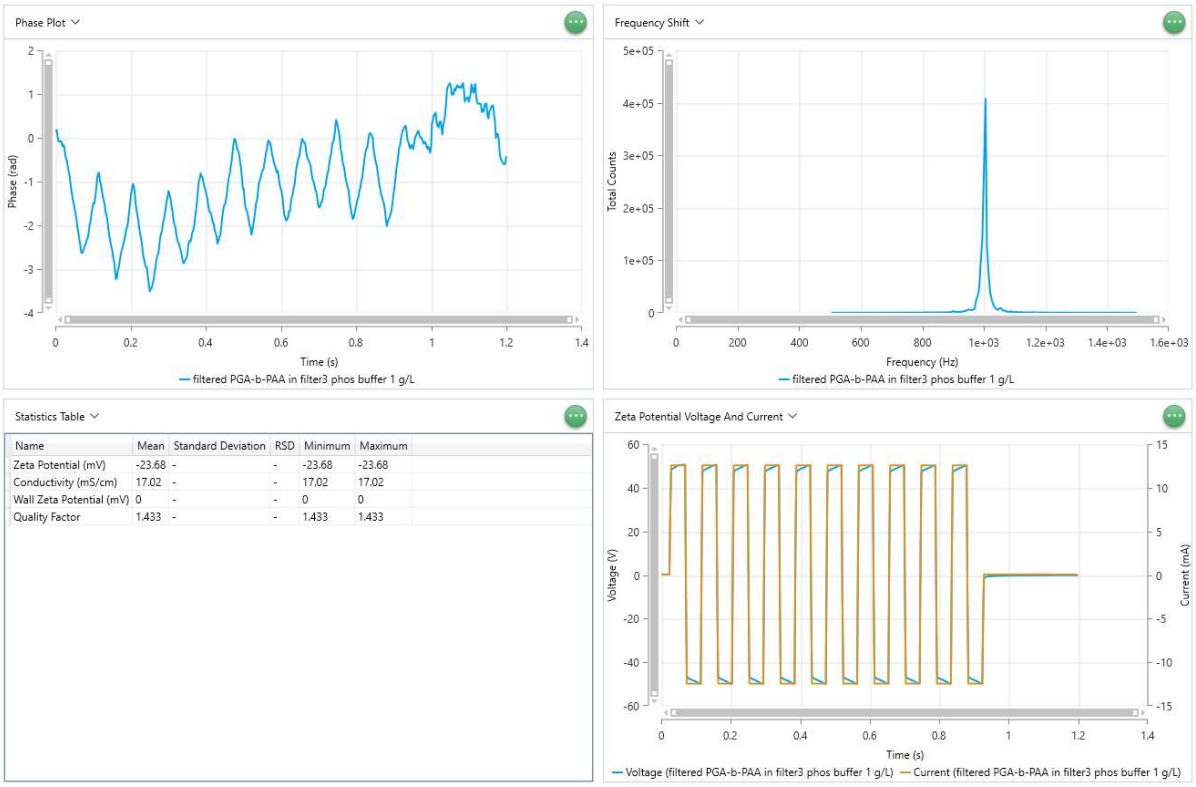

Figure 22: ζ-potential measurement of PGA-b-PAA (1 g·L^{-1}) in a pH 12 phosphate buffer.

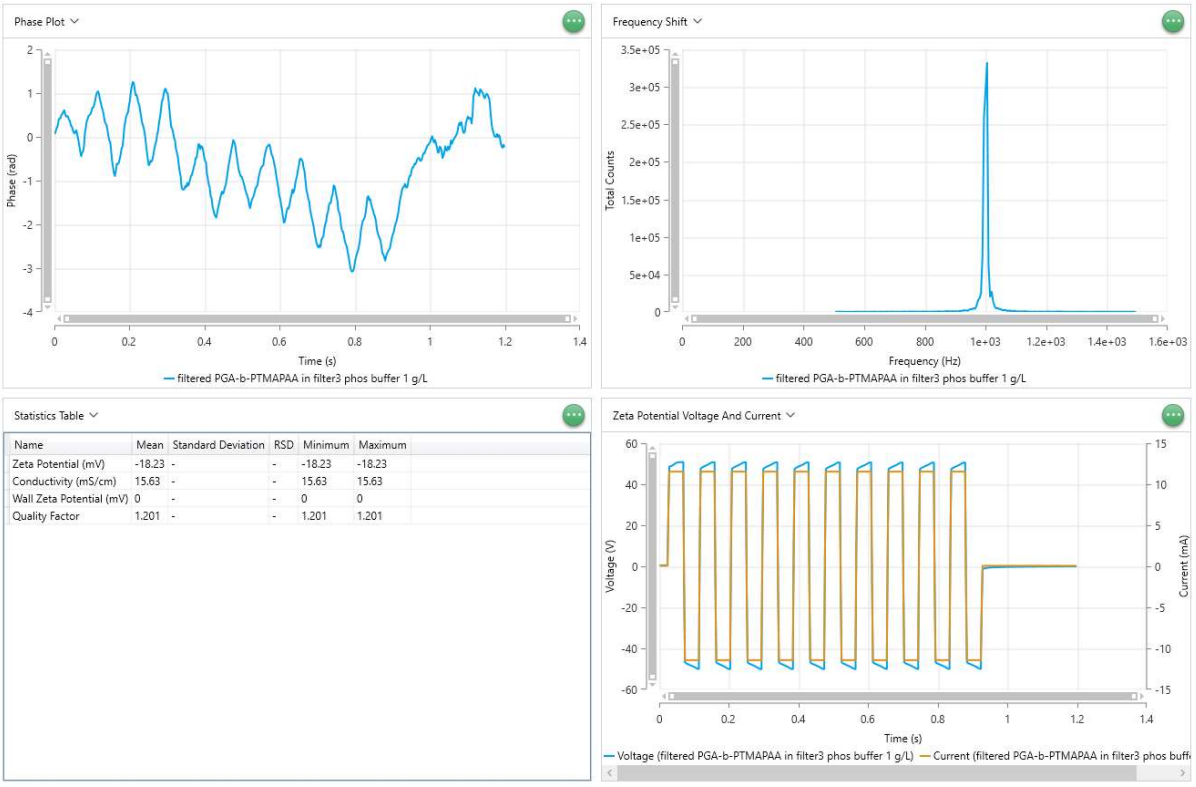

Figure 23: ζ-potential measurement of PGA-b-PDMAPAA (1 g·L^{-1}) in a pH 12 phosphate buffer.

6.5 AFM data

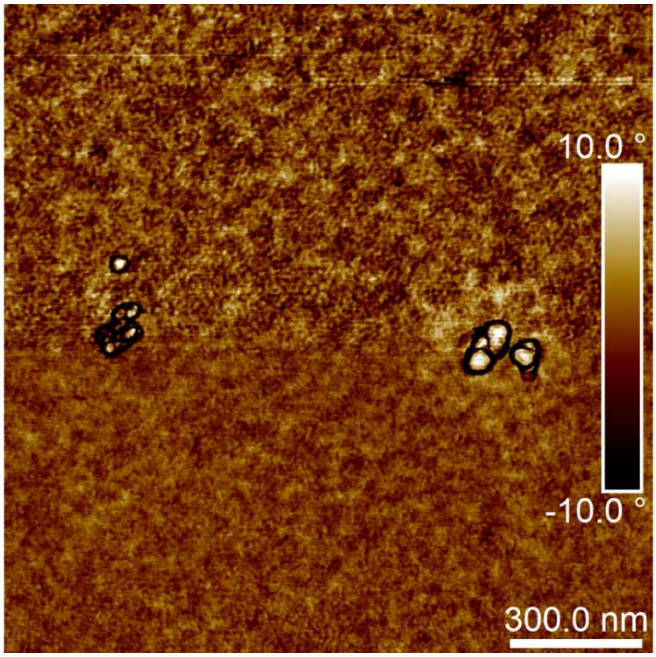

Figure 24: AFM phase image corresponding with the AFM height image in Figure 17a.

Table 3: Statistical analysis of the nanoparticles found using AFM.

Particle	Diameter (nm)	Height (nm)
1	77	18
2	72	18
3	79	26
4	51	17
5	71	10
6	58	20
7	51	20
8	60	6
9	59	12
10	61	12
Mean	64	16
Standard deviation	10	6
Confidence interval	6	4